PAPER

Syntheses and reductions of *C*-dimesitylboryl-1,2-dicarba-*closo*-dodecaboranes†‡

Jan Kahlert,[a] Lena Böhling,[a] Andreas Brockhinke,[a] Hans-Georg Stammler,[a] Beate Neumann,[a] Louis M. Rendina,[b] Paul J. Low,[c] Lothar Weber*[a] and Mark A. Fox*[d]

Two *C*-dimesitylboryl-1,2-dicarba-*closo*-dodecaboranes, 1-(BMes$_2$)-2-R-1,2-C$_2$B$_{10}$H$_{10}$ (**1**, R = H, **2**, R = Ph), were synthesised by lithiation of 1,2-dicarba-*closo*-dodecaborane and 1-phenyl-1,2-dicarba-*closo*-dodecaborane, respectively, with *n*-butyllithium and subsequent reaction with fluorodimesitylborane. These novel compounds were structurally characterised by X-ray crystallography. Compounds **1** and **2** are hydrolysed on prolonged exposure to air to give mesitylene and boronic acids 1-(B(OH)$_2$)-2-R-1,2-C$_2$B$_{10}$H$_{10}$ (**3**, R = H, **4**, R = Ph respectively). Addition of fluoride anions to **1** and **2** resulted in boryl-carborane bond cleavage to give dimesitylborinic acid HOBMes$_2$. UV absorption bands at 318–333 nm were observed for **1** and **2** corresponding to local π−π*-transitions within the dimesitylboryl groups while visible emissions at 541–664 nm with Stokes shifts of 11 920–16 170 cm^{-1} were attributed to intramolecular charge transfer transitions between the mesityl and cluster groups. Compound **2** was shown by cyclic voltammetry to form a stable dianion on reduction. NMR spectra for the dianion [**2**]$^{2-}$ were recorded from solutions generated by reductions of **2** with alkali metals and compared with NMR spectra from reductions of 1,2-diphenyl-*ortho*-carborane **5**. On the basis of observed and computed ^{11}B NMR shifts, these *nido*-dianions contain bowl-shaped cluster geometries. The carborane is viewed as the electron-acceptor and the mesityl group is the electron-donor in *C*-dimesitylboryl-1,2-dicarba-*closo*-dodecaboranes.

Introduction

Tri-coordinate boron compounds have been intensely investigated in the past two decades in view of potential applications as functional materials.[1] The most widely employed functional moiety containing a tri-coordinate boron atom is the dimesitylboryl group (BMes$_2$; Mes = 2,4,6-Me$_3$C$_6$H$_2$) in which the unsaturated boron centre is kinetically stabilised by steric shielding of the mesityl groups. The empty p$_z$-orbital at the boron atom can interact with the π-system of attached organic skeletons

[a]*Fakultät für Chemie der Universität Bielefeld, 33615 Bielefeld, Germany.*
E-mail: lothar.weber@uni-bielefeld.de
[b]*School of Chemistry, The University of Sydney, Sydney, NSW 2006, Australia*
[c]*School of Chemistry and Biochemistry, University of Western Australia,*
35 Stirling Highway, Crawley, Perth 6009, Australia
[d]*Department of Chemistry, Durham University, Durham DH1 3LE, UK.*
E-mail: m.a.fox@durham.ac.uk

which leads to a narrowing of the HOMO–LUMO-gap (HLG) by lowering the LUMO energy. Indeed, the π-acceptor strength of the BMes$_2$ group is similar to those of cyano-[2] and nitro-[3] groups. These electronic characteristics have led to organic materials containing BMes$_2$ units finding application as electron-transporting materials in opto-electronic devices.[4,5] Compounds containing BMes$_2$ can be strongly fluorescent and thus have been used in organic light emitting diodes (OLEDs).[5,6] Moreover, the ability of the boron atom to form selectively covalent adducts with small anions has led to applications of these compounds as colorimetric and luminescent sensors for fluoride[7–9] and cyanide.[10,11]

Other boron-containing compounds that have gained considerable interest in the last seven years in the field of opto-electronic materials are derivatives of the dicarba-*closo*-dodecaborane isomers (1,2-, 1,7- and 1,12-C$_2$B$_{10}$H$_{12}$ which are *ortho*-, *meta*- and *para*-carborane, respectively).[12,13] Due to their delocalised σ-electron systems ('3D aromaticity'), these clusters possess high thermal and chemical stabilities.[14] The *ortho*-carborane is a unique electron-acceptor when connected to a donor at one or both cluster carbon atoms (at C1 and/or C2 in 1,2-C$_2$B$_{10}$H$_{12}$) due to the elasticity of the cluster C1–C2 bond.[15–17] The *ortho*-carborane unit thus can play an active role as the acceptor in donor–acceptor molecules (dyads).
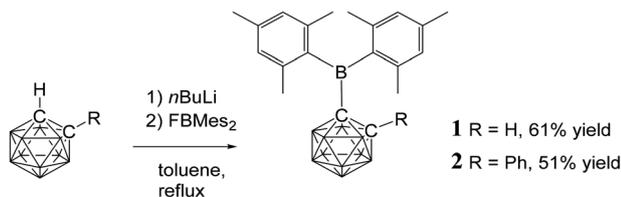
Fig. 1 Syntheses of the novel *C*-dimesitylboryl-*ortho*-carboranes **1** and **2**.

Photoexcitation of such dyads induces a charge transfer from an organic scaffold to the carborane cluster which either led to luminescence quenching[18] or to charge transfer (CT) emissions or both depending on the solvents used[19–21] and whether the materials were investigated as solids.[22–28] Compounds with both BMes$_2$ and *ortho*-carboranyl groups are known with *para*-phenylene bridges linking both units.[29,30] In these systems, the *ortho*-carboranyl group served as a strongly inductive electron-withdrawing group as the cluster increased the Lewis acidity of the triarylborane as found by fluoride ion titrations compared to the triarylborane without the cluster attached.[29] Another compound containing both BMes$_2$ and *ortho*-carboranyl group was reported with an ethylene bridge linking both units.[31]

Of the few *ortho*-carboranes with tri-coordinate boron substituents at their carbon atoms reported,[24–26,32–36] only *C*-benzodiazaborolyl-*ortho*-carboranes have been investigated regarding their photophysical, electrochemical and spectro-electrochemical properties.[25] However, the benzodiazaborolyl group generally acts as a π-donor and is therefore electronically quite distinct from the BMes$_2$ moiety. In order to better understand the photophysical and electrochemical properties of *ortho*-carboranes with boryl groups, studies with compounds containing a tri-coordinate boron π-acceptor would be appealing and allow one to determine more precisely the electronic interplay between the carborane and tri-coordinate boron electron-withdrawing units. Therefore we present herein, the syntheses and crystal structures of two *ortho*-carborane derivatives **1** and **2** with a BMes$_2$ group at one of the cage carbon atoms and their photophysical and electrochemical properties (Fig. 1). The geometry of the reduced species of **2** was also determined by a combination of ^{11}B NMR spectroscopy and GIAO-NMR DFT computations.

Results and discussion

Syntheses and characterisation of 1 and 2

Compounds **1** and **2** were synthesised by reaction of fluorodimesitylborane with the corresponding *C*-lithiocarborane, generated *in situ* by metallation of *ortho*-carborane and 1-phenyl-*ortho*-carborane, in boiling toluene (Fig. 1). The elevated temperatures proved to be essential as no conversion was observed at ambient temperature. Purification was achieved by aqueous work-up and the target compounds were isolated in moderate

yields by crystallisation from *n*-hexane/dichloromethane mixtures. The elemental analytical result for **1** was significantly lower (0.8% for carbon) than the calculated value. Similar discrepancies have been noted elsewhere for related compounds.[33] It is possible that the formation of boron carbide during the combustion analysis may adversely affect the values obtained.

Signals in the ^{11}B{^{1}H} NMR spectra of **1** and **2** between 3.7 and −12.9 ppm confirm the presence of the *ortho*-carborane clusters. The ^{11}B peaks at 78.9 ppm (**1**) and 80.4 ppm (**2**) are assigned to the BMes$_2$ groups and are very broad compared to the peaks corresponding to the cluster. The ^{11}B chemical shifts of the Mes$_2$B groups in **1** and **2** are virtually identical to trimesitylborane (79.2 ppm) and phenyldimesitylborane (79.3 ppm).[37] Thus, the *ortho*-carboranyl groups influence the chemical shift of the tri-coordinate boron atom of the BMes$_2$ unit in the same manner as a phenyl or mesityl substituent.

Hydrolyses of 1 and 2

Since aqueous work-ups were used in the preparation of **1** and **2** these *C*-boryl-*ortho*-carboranes are considered to be water-stable – unlike many reported *C*-boryl-*ortho*-carboranes that could not be isolated pure due to facile hydrolysis.[32] The ^{1}H and ^{11}B NMR spectra for **1** and **2** in deuterated chloroform solutions containing excess water also showed no changes. The sterics of the mesityl and the carboranyl groups appear to prevent facile hydrolysis of the boron atom in **1** and **2**.

Solids of **1** and **2** do, however, hydrolyse on prolonged exposure to air (complete conversion after three weeks for **1** and eighteen months for **2**) to give mesitylene and the new carboranylboronic acids, **3** and **4** (Fig. 2). While these acids could not be obtained pure, they were identified by multinuclear NMR spectroscopy and mass spectrometry. The observed cleavage of the B–C(mesityl) bond in the process is not without precedent. It has been shown elsewhere that mesitylene is formed from the reaction of dimesitylborinic acid, Mes$_2$BOH, with trimethylaluminium.[38] The initial steps in these air-induced hydrolyses of **1** and **2** probably involve cleavage of the B–C(mesityl) bonds by oxygen (as in the B–C
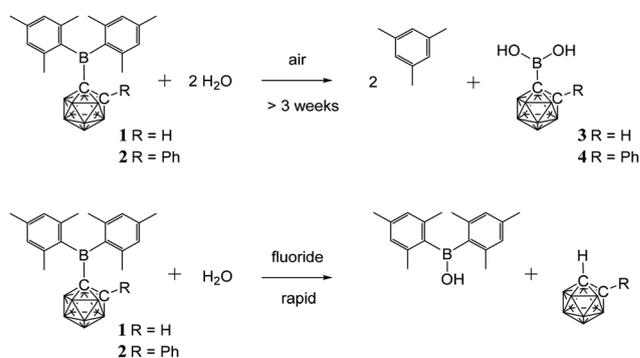

Fig. 2 Hydrolysed products from reactions of **1** and **2** with air and fluoride ions.

(phenyl) bond cleavage reaction of triphenylboron by oxygen[39]) followed by hydrolysis with traces of water present in air.

As many organic dimesitylboranes have been explored as fluoride sensors,[7,29] the reactivity of **1** and **2** towards fluoride ions was of interest. Chloroform solutions of **1** and **2** were treated with an excess of tetra-*n*-butylammonium fluoride hydrate (TBAFH) while acetonitrile solutions of **1** and **2** were added with potassium fluoride (KF) and 18-crown-6 to obtain the desired fluoride adducts [**1**·F]⁻ and [**2**·F]⁻, respectively, where the fluoride ion is bound to the boryl boron atom. Hydrolysis took place instead in all cases to give Mes$_2$BOH, and the corresponding unsubstituted carborane, 1,2-C$_2$B$_{10}$H$_{12}$ or 1-Ph-1,2-C$_2$B$_{10}$H$_{11}$, as detected by ¹H, ¹¹B, ¹³C and ¹⁹F NMR spectroscopies on the reaction mixtures (Fig. 2). These reactions were complicated by fluoride-ion deboronation processes on the unsubstituted carboranes to give ¹¹B and ¹⁹F NMR peaks corresponding to fluoroborates of the boron atom initially removed from the cluster.[40]

It is possible that fluorodimesitylborane, Mes$_2$BF, is initially formed in the reaction as Mes$_2$BF is known to be easily hydrolysed to Mes$_2$BOH.[39,41] However, careful ¹⁹F NMR monitoring of the reaction mixtures from **1** and **2** with TBAFH in the first few minutes did not reveal any evidence of an intermediate such as the fluoride adducts [**1**·F]⁻, [**2**·F]⁻ or Mes$_2$BF. The reactions of potassium hydroxide (KOH) and 18-crown-6 with **1** and **2** in acetonitrile gave Mes$_2$BOH and the corresponding unsubstituted carborane. Deboronation products were also present in the latter reactions as the combination of KOH and 18-crown-6 is a strong deboronating agent.[42]

X-ray crystallography

Single crystals of **1** and **2** were grown from *n*-hexane/dichloromethane mixtures and their molecular structures were determined by X-ray diffraction (Fig. 3 and 4, Table 1). The BMes$_2$
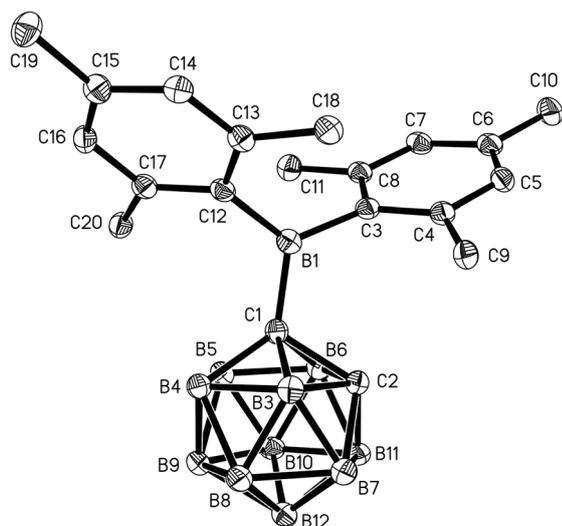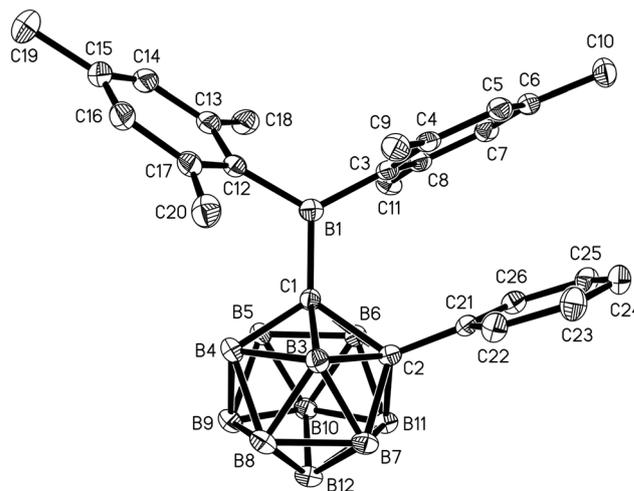

Fig. 4 Molecular structure of **2** with hydrogen atoms omitted. Thermal ellipsoids are plotted at 50% probability.

Table 1 Selected bond lengths and angles for **1** and **2**

	1		**2**	
	Exp.	Calcd.[a]	Exp.	Calcd.[a]
Bond lengths [Å]				
C1–C2	1.677(3)	1.671	1.761(2)	1.791
C1–B1	1.635(3)	1.641	1.629(2)	1.648
C1–B3	1.728(3)	1.723	1.727(2)	1.724
C1–B6	1.756(3)	1.757	1.748(2)	1.751
B1–C3	1.595(3)	1.601	1.590(2)	1.597
B1–C12	1.581(3)	1.593	1.602(2)	1.602
Bond angles [°]				
C1–B1–C3	115.7(2)	116.9	118.2(1)	120.7
C1–B1–C12	121.0(2)	121.0	119.4(1)	118.3
C3–B1–C12	123.3(2)	122.2	122.4(1)	120.9
Torsion angles [°]				
C2–C1–B1–C3	36.0(2)	34.9	22.5(2)	37.1
C2–C1–B1–C12	−144.5(2)	−145.1	−157.8(2)	−145.8
B3–C1–B1–C3	102.7(2)	102.1	95.8(2)	110.6
B3–C1–B1–C12	−77.8(2)	−77.8	−84.5(2)	−72.3
Interplanar angles [°]				
(C1,B1,C3,C12)(C3–C8)	77.9(1)	74.2	78.6(1)	69.8
(C1,B1,C3,C12)(C12–C17)	54.1(1)	58.3	65.5(1)	64.0

[a] Calculated values from optimised geometries of **1** and **2** at B3LYP/6-31G*.

groups adopt orientations with C2–C1–B1–C3 torsion angles at 36.0(2)° and 22.5(2)° and C2–C1–B1–C12 at −144.5(2)° and −157.8(2)° in **1** and **2** respectively (Table 1). Thus the empty p$_z$-orbitals are approximately in plane with the C1–B3 bonds in the clusters and these C1–B3 bonds are shorter than the C1–B6 bonds by 0.02–0.03 Å in both compounds. However, all B–B and B–C bonds lengths in the clusters are within the usual range.[24]

The C1–C2 distance of 1.677(3) Å in **1** agrees within 3 esd with C1–C2 bond lengths of 1.667(1)–1.673(1) Å found in other *C*-monoboryl-*ortho*-carboranes.[24,33,36] By contrast, the C1–C2

Fig. 3 Molecular structure of **1** with hydrogen atoms omitted for clarity. Thermal ellipsoids are drawn at 50% probability.

bond of 1.761(2) Å in **2** is significantly longer than in its 1,3-diethyl-1,3,2-benzodiazaborol-2-yl analogue (1.701(2)–1.730(2) Å),[24] in 1,2-diphenyl-*ortho*-carborane (1.720(4)–1.733(4) Å)[43] and 1,2-diboryl-*ortho*-carboranes (1.695(1)–1.725(2) Å).[26,36] The longer C1–C2 bond in **2** is explained by the different steric interactions between the BMes$_2$ group at C1 and the phenyl ring at C2 in **2**.

The BMes$_2$ groups are linked to the cage carbon atoms by B–C single bonds (C1–B1) with lengths of 1.635(3) Å in **1** and 1.629(2) Å in **2**, which is at the upper edge of the range determined for other *C*-boryl-*ortho*-carboranes (1.607(4)–1.649(12) Å).[24–26,33,36] The B–C bond lengths between the mesityl rings and the boryl-boron atoms (B1–C3/C12 1.581(3)–1.602(2) Å) are typical for dimesitylboranes. As a consequence of the three-dimensional shape of the cluster in both structures, the interplanar angle enclosed by the mesityl ring pointing towards the second cage carbon atom and the plane defined by the boryl-boron atoms and the three neighbouring carbon atoms (77.9(1)° (**1**), 78.6(1)° (**2**)) is larger than in most reported structures of BMes$_2$ compounds.[44] A virtually perpendicular orientation of the phenyl substituent in **2** with respect to the C1–C2 axis (torsion angles = C1–C2–C21–C22 94.3(2)°, C1–C2–C21–C26 −91.5(2)°) corresponds to the situation in other disubstituted phenyl-*ortho*-carboranes and is preferred due to sterics.[43,45]

Photophysics

Photophysical data for **1** and **2** are listed in Table 2. The absorption maxima of both *C*-dimesitylboryl-*ortho*-carboranes (Fig. S1‡) in solvents of different polarity do not display any significant solvatochromism. The lack of solvatochromism points to very similar dipole moments in the electronic ground state and the initial excited state indicating that local transitions within the dimesitylboryl unit give rise to the absorption bands observed. The presence of the phenyl ring at C2 in **2** appears to lower the HOMO–LUMO energy gap as the absorption maxima of **2** (330 nm–333 nm) are bathochromically shifted by approximately 12–14 nm compared to **1** (318–319 nm) in all solvents used. The energy difference in the absorption maxima between **1** (329 nm) and **2** (332 nm) in the solid state is smaller.

Emission maxima of both compounds in cyclohexane are virtually identical at 541 nm for **1** and 544 nm for **2** with large Stokes shifts of 12 300 cm^{-1} for **1** and 11 920 cm^{-1} for **2**. The luminescence spectra (Fig. 5) reveal positive solvatochromism with emission maxima in the more polar solvent dichloromethane in the red emission region at 664 nm for **1** and 643 nm for **2**. By using the Lippert–Mataga method[46,47] with an Onsager radius of 4.00 Å estimated from the molecular structures, the calculated transition dipole moments are 10.4 D (**1**)

Table 2 Photophysical data for **1** and **2**. CyH = cyclohexane, THF = tetrahydrofuran, DCM = dichloromethane[a]

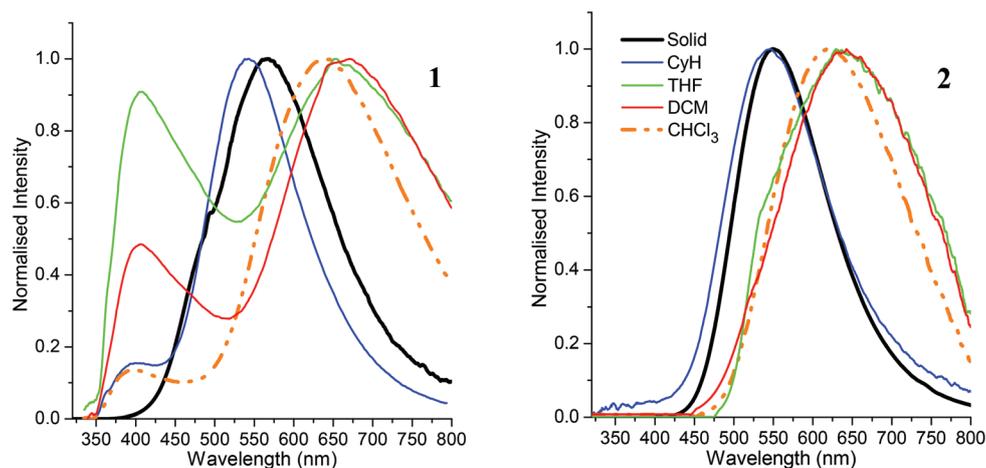|		Solid	CyH	CHCl$_3$	THF	DCM
Absorption λ_{max} [nm] (ε)[a]	1	329	318 (8300)	319 (7350)	319 (7060)	318 (7920)
	2	332	332 (6750)	331 (7330)	333 (5710)	330 (7760)
Emission λ_{max} [nm] (relative height)	1	567	400, 541 (0.15 : 1)	396, 641 (0.14 : 1)	408, 653 (0.91 : 1)	406, 664 (0.48 : 1)
	2	550	544	620	640	643
Stokes shift [cm^{-1}]	1	12 310	5500, 12 300	5780, 15 610	6240, 15 600	6600, 16 170
	2	9210	11 920	14 310	14 660	14 800

[a] In L mol^{-1} cm^{-1}.

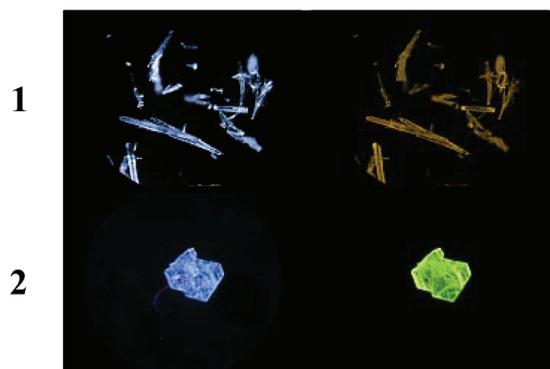**Fig. 5** Emission spectra of **1** and **2** in the solid state and in various solvents.

Fig. 6 Crystals of **1** and **2**. Left column: Without UV irradiation. Right column: Under UV irradiation at 350 nm.
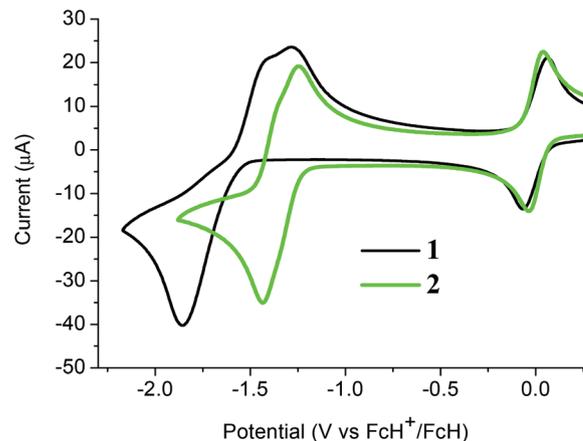

Fig. 7 Cyclic voltammograms of **1** and **2** with a glassy carbon working electrode in acetonitrile and internal ferrocenium/ferrocene couples at 0.0 V.

and 9.2 D (**2**) – similar to transition dipole moments of *C*-benzodiazaborolyl-*ortho*-carboranes (6.9–10.9 D).[24–26] The results show that the carborane cluster plays a part in the emission process acting as the electron acceptor of the charge transfer process after excitation. The solid-state emissions occur at longer wavelengths than in cyclohexane (Fig. 6). This bathochromic shift is more pronounced for **1** (567 nm) than for **2** (550 nm) and is presumably caused by fluorophore–fluorophore interactions. The quantum yields (Φ) are very low in all solvents (<1%) with higher values of 2% (**1**) and 7% (**2**) found in the solid state.

In addition to these low-energy emissions, compound **1** displays a weaker emission band at the violet edge of the visible spectrum in polar solvents. The high-energy emissions with smaller Stokes shifts of 5500–6600 cm^{-1} probably originate from local transitions at the BMes$_2$ group.[48] Similar dual emissions originating from both local and CT transitions have been reported for some *ortho*-carboranes with substituents at one or both cluster carbon atoms.[20,24–27]

Electrochemistry

The electrochemical properties of both *C*-dimesitylboryl-*ortho*-carboranes **1** and **2** were investigated by cyclic voltammetry (CV, Fig. 7). The peak potentials measured in acetonitrile and dichloromethane solutions, with platinum and glassy carbon working electrodes are listed in Table S1.‡ The traces resemble reported CV data on reductions of carboranes elsewhere[20,21,25–27,49–54] and, by inference, reductions take place at the carborane clusters in **1** and **2**. CV traces for reductions of the BMes$_2$ group would involve a simple one-electron reversible wave. In contrast, the one-electron reduction wave associated with PhBMes$_2$ occurs at −2.30 V (*vs.* the ferrocenium/ferrocene couple at 0.0 V)[2] and hence the BMes$_2$ localised reduction in **1** and **2** likely falls outside the electrochemical window examined here.

A CV trace for *ortho*-carborane or a *C*-monosubstituted-*ortho*-carborane usually shows a two-electron cathodic wave and an anodic wave that is not of the same current intensity as the cathodic wave.[25,49,50] Often the peak–peak separation

between the cathodic and anodic peaks of the wave can be several hundred millivolts due to the structural rearrangement of the dianion on the CV timescale. Decomposition and proton-coupled electron transfer (PCET) processes can also complicate the electrochemical response.[49,55]

The CV of **1** in acetonitrile with a glassy carbon working electrode shows a two-electron cathodic wave at −1.86 V and two anodic waves at −1.43 V and −1.29 V with values referenced to the ferrocenium/ferrocene redox couple at 0 V (Fig. 7). The cathodic wave value of −1.80 V for **1** means that **1** is more easily reduced than *C*-monophenyl-*ortho*-carborane at −2.25 V[50] reflecting the substantial electron-withdrawing effect of the BMes$_2$ group. Similar CV traces are observed for **1** with a platinum working electrode and with DCM as solvent (Fig. S2 and Table S1‡). The non-equivalent current intensities between the forward and reverse waves for **1** suggest that the dianion $[\mathbf{1}]^{2-}$ is not stable and would be difficult to isolate.

A CV trace for *ortho*-carborane with aryl substituents at both cluster carbon atoms generally shows a reversible wave (or two) on reduction.[20,25–27,49,51–54] In several cases, a stepwise reduction involving two separated one-electron reduction steps has been found, with the initial reduction process giving rise to a radical anion with an unusual $2n + 3$ skeletal electron (SE) count. One example is diphenyl-*ortho*-carborane **5** where the radical anion has been shown to be stable enough to be observed spectroscopically at ambient temperature in solution (Fig. 8).[51] The first one-electron reduction process on the CV
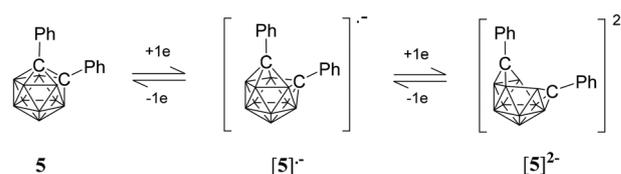

Fig. 8 Two one-electron reductions for 1,2-diphenyl-*ortho*-carborane **5**.

timescale is usually slow due to the rearrangement of the cluster and is often immediately followed by a second one-electron process giving an apparently two-electron cathodic wave. The latter wave is usually evident in DCM for these carboranes.[26] However, on back oxidation two separate anodic waves (with the combined current intensities similar to the current intensity of the cathodic wave) are evident corresponding to two one-electron processes.[25,26]

The CV of **2** in acetonitrile here shows two very closely spaced and barely resolved one-electron waves (Fig. 7). These waves are separated by less than 80 mV based on gaussian analyses of square-wave potential traces (Fig. S3‡). The two half-wave potentials are estimated to be −1.31 and −1.39 V which indicate that **2** is reduced more readily than diphenyl-*ortho*-carborane **3** at −1.57 and −1.72 V under the same CV conditions. Thus, compound **2** does form a radical anion with a $2n + 3$ skeletal electron count. However, the very low comproportionation constant (K_c) associated with the intermediate $[2]^{\cdot-}$ means that spectroscopic observation is challenging, and the monoanion could not be isolated in any appreciable concentration in the comproportionated mixture obtained following one-electron reduction (Fig. S4‡). The CV of **2** in DCM shows the expected CV pattern with a one two-electron cathodic wave and two one-electron anodic waves (Fig. S2 and Table S1‡).

Computations

Calculated bond lengths and angles from geometries of **1** and **2** optimised at B3LYP/6-31G* are in good agreement with the experimental values (Table 1). The lengthening of the C1–B6 bonds compared to the C1–B3 bonds is attributed to steric repulsion between an *ortho*-methyl group of one of the mesityl rings and the B6–H unit. Computed energy barriers for the rotation around the C1–B1 bonds are 6.1 kcal mol^{-1} in **1** and 18.6 kcal mol^{-1} in **2**. Comparison between computed GIAO-NMR and experimental ^{11}B NMR chemical shifts for **1–4** are in very good agreement (Table S2‡).

The HOMO is a combination of π-orbitals at the mesityl groups (π(Mes)) and the LUMO consists mainly of the empty p-orbital of the boryl boron atom (p(B)) (Fig. 9). Antibonding orbitals with significant cluster contributions have much higher energies (>−0.16 eV) and thus the influence of the clusters on the absorption process is merely inductive in both cases. According to TD-DFT calculations π(Mes)–p(B) transitions with oscillator strengths (f) of 0.0065 to 0.0698 can be assigned to the absorption bands of both compounds (Tables S3 and S4‡). Therefore, the electron density in the initially formed excited state is shifted within the BMes$_2$-unit only which is not expected to entail strong changes in the overall dipole moment. This is in agreement with the lack of solvatochromism in the absorption spectra. Weak transitions between the π-orbitals of the phenyl group of **2** and the p(B) orbital as well as π–π* transitions within the phenyl ring occur at considerably higher energy far in the UV region. The HOMO–LUMO gap energy of **2** is 0.10 eV smaller than that in **1** which
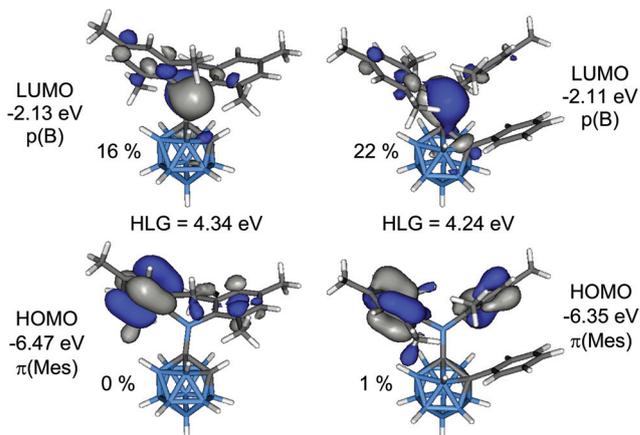

Fig. 9 Frontier molecular orbitals of **1** (left) and **2** (right). The percentage values are the cluster contributions to the molecular orbitals.

agrees well with the observed bathochromic shift of the absorption maximum of **2** compared to **1**.

In order to elucidate the origin of the visible CT emission of **1** and **2**, their geometries were optimised at the first excited singlet state (S$_1$). In both cases "open" cluster geometries were found with C1–C2 distances expanded to 2.384 Å (**1**) and 2.440 Å (**2**), respectively. The frontier orbitals of the S$_1$ geometries are depicted in Fig. 10. These orbitals were calculated at the ground state, S$_0$ thus HOMO and LUMO correspond to the highest and second highest singly occupied orbitals in the S$_1$ state. The HOMO is a π(Mes) orbital but the LUMO, in contrast, is an antibonding cluster orbital (cage*) with small contributions from the exopolyhedral boron atom (**1**: 15%, **2**: 8%). Thus, the HOMO–LUMO transition corresponds to a charge transfer between the cluster and the mesityl groups from the excited state and the two compounds can be regarded as donor–acceptor systems. TD-DFT calculations predicted low-
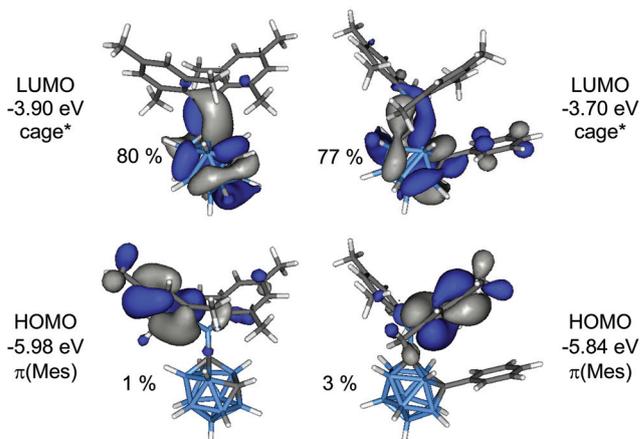

Fig. 10 Frontier orbitals of the S$_1$ geometries of **1** (left) and **2** (right). The percentage values are the cluster contributions to the molecular orbitals.

Table 3 Calculated fluoride ion affinities in kcal mol^{-1} for **1**, **2** and related XBMes$_2$ compounds in order of decreasing strengths

| X	Reference	Fluoride ion affinity
1-(1,2-C$_2$B$_{10}$H$_{11}$)– (**1**)	This work	132.9
1-(2-Ph-1,2-C$_2$B$_{10}$H$_{10}$)– (**2**)	This work	127.3
4-(1'-(2'-Me-1',2'-C$_2$B$_{10}$H$_{10}$))C$_6$H$_4$–	29	123.9
4-(1'-(2'-Ph-1',2'-C$_2$B$_{10}$H$_{10}$))C$_6$H$_4$–	29	122.6
4-Mes$_2$BC$_6$H$_4$–	9	119.2
Ph–	11	113.2

energy emissions with low oscillator strengths at 859 nm (**1**; f = 0.0016) and 783 nm (**2**; f = 0.0066) for these transitions and gave the same trend as experimentally observed with **1** emitting at longer wavelength than **2**.

The geometries of the fluoride adducts [**1**·F]$^-$ and [**2**·F]$^-$ were optimised in order to examine why fluoride adducts were not observed experimentally. The fluoride ion affinities of **1** and **2** are 132.9 and 127.3 kcal mol^{-1}, respectively, which are higher than the fluoride ion affinities of many aryldimesityl-boranes (Table 3).[8] Although the strong carborane electron-withdrawing character increases the affinities for the fluoride ion in **1** and **2** with respect to the affinities of the aryldimesityl-borane analogues, the optimised geometries [**1**·F]$^-$ and [**2**·F]$^-$ contain unusually long B–C(carboranyl) bonds of 1.786 and 1.823 Å respectively. These bond lengths suggest that they would be easily cleaved either before the B–F bond is formed or by hydrolysis as observed experimentally.

Geometries of the dianions [**2**]$^{2-}$ and [**5**]$^{2-}$

While *closo*-dicarbadodecaboranes all adopt the pseudo-icosahedral geometry, several different geometries of *nido*-dicarbadodecaborane dianions have been determined crystallographically (Fig. 11).[56] Dianions with almost planar C$_2$B$_4$ open faces like [**6**]$^{2-}$ and [**7**]$^{2-}$ are observed in Group 1 metallacarboranes.[57–60] Bowl-shaped geometries have been observed in carborane dianions like [**8**]$^{2-}$ and [**9**]$^{2-}$ with tethers at both cage carbons.[59,61] The bowl geometry in [**9**]$^{2-}$ differs from that in [**8**]$^{2-}$ where [**9**]$^{2-}$ has a notably smaller open face.[61] These bowl-shaped geometries are similar to geometries determined for neutral 12-vertex tetracarbadodecaboranes by X-ray crystallography.[62] The neutral compound **10** may also be regarded as a genuine 12-vertex dicarbadodecaborane dianion [R$_2$C$_2$B$_{10}$H$_{10}$]$^{2-}$ with two positively charged phosphonium groups.[63]

While there are several structural studies published on *nido*-dicarbadodecaborane dianions, the geometries of *nido*-dicarbadodecaborane dianions in solutions have not been determined. The successful method[64] of comparing observed and computed ^{11}B NMR data to determine carborane cluster geometries is applied here for dianion [**2**]$^{2-}$. Before discussing the dianion [**2**]$^{2-}$ made by chemical reductions on **2**, the dianion [**5**]$^{2-}$ generated from diphenyl-*ortho*-carborane **5** is described here to demonstrate the use of the combined experimental and calculated ^{11}B NMR method in determining the geometry of its dianion. Dianion [**5**]$^{2-}$ has been proposed to
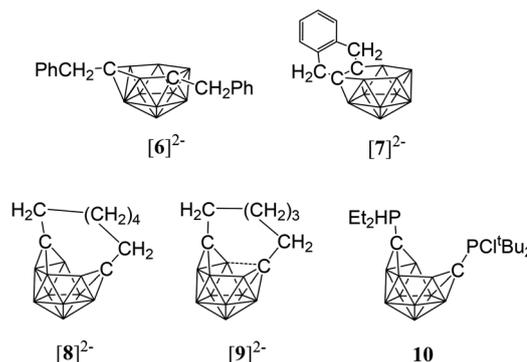
Fig. 11 Geometries of *nido*-dicarbadodecaboranes determined by X-ray crystallography.
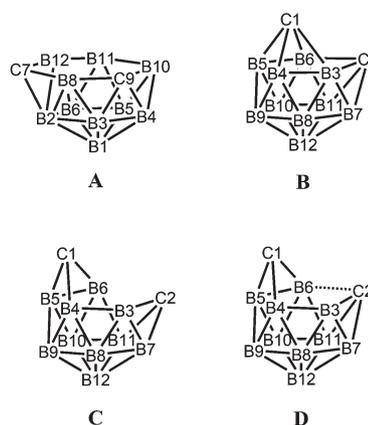
Fig. 12 Geometries **A–D** of *nido*-dicarbadodecaborane dianions with atom numbering.

have a geometry[65] with a C$_2$B$_4$ open face **A** or a geometry[54,66] with a C$_2$B$_2$ open face **B** (Fig. 12). Thus, the geometry of the dianion [**5**]$^{2-}$ has not been established even though this dianion has been known for many decades.[67]

Chemical reductions of **5** were carried out with alkali metals (Li, Na, K) in THF solutions. The reactions were monitored by ^{11}B NMR spectroscopy until all the peaks corresponding to the starting carborane and the red colours of the solutions due to the radical monoanions disappeared. The ^{11}B {^{1}H} spectra of the dianions [**5**]$^{2-}$ in clear yellow solutions show 2 : 2 : 4 : 2 patterns which are not significantly influenced by the different alkali metal cations (Fig. 13). This pattern suggests a geometry of high symmetry or two mirror-image geometries that are fluctional in solution for [**5**]$^{2-}$ with the metal cations not strongly interacting in solution.

Geometry optimisations on [**5**]$^{2-}$ reveal that the bowl-shaped geometry **C** is more stable than **A** and **B** by 5.5 and 11.0 kcal mol^{-1} respectively. More importantly, the computed GIAO ^{11}B NMR chemical shifts of the bowl-shaped geometry fit well with observed shifts when fluctionality between the two mirror-image geometries of **C** takes place in solution (Table 4).
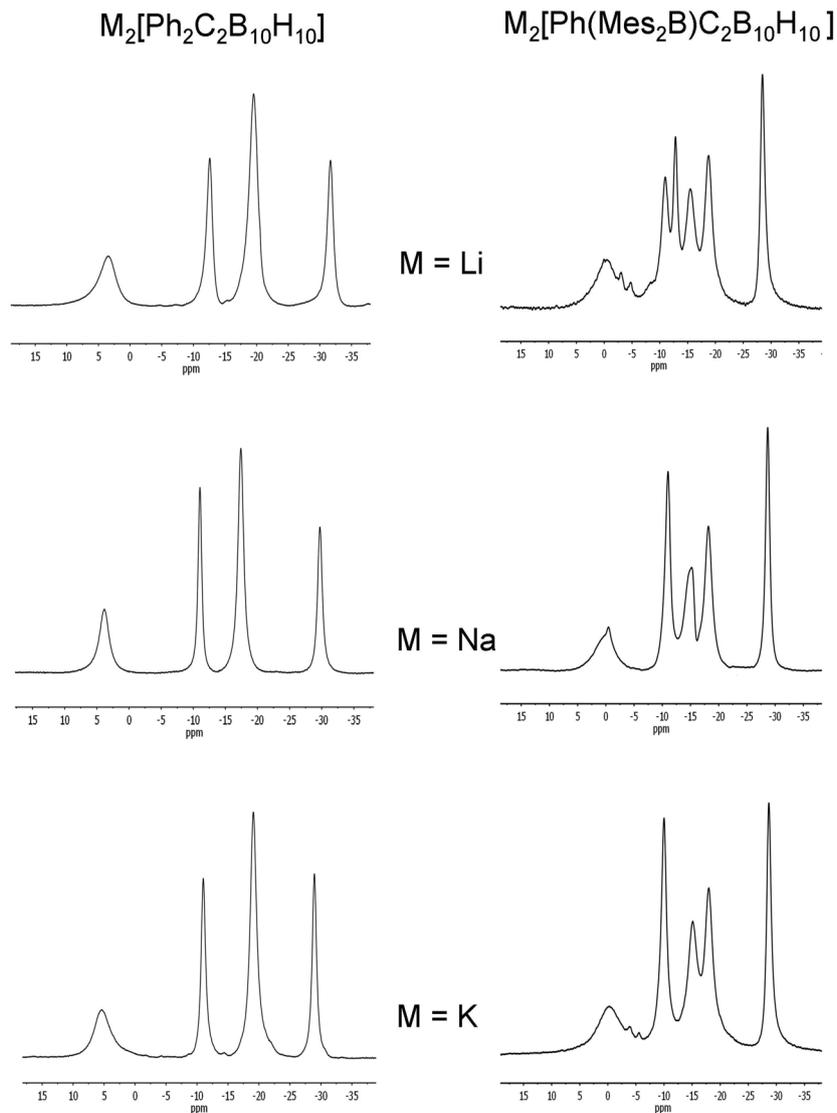
Fig. 13 $^{11}B\{^1H\}$ NMR spectra of $M_2[5]^{2-}$ and $M_2[2]^{2-}$ (M = Li, Na or K) in THF. The broad peaks at 65–70 ppm corresponding to the boryl boron in $[2]^{2-}$ are not shown here.

The geometry **D** found in $[9]^{2-}$ could not be located for $[5]^{2-}$ where the initial geometry **D** rearranged to **C** on optimisation.

Reduction of **2** with sodium metal in 1,2-dimethoxyethane (DME) yielded a dark red solid identified as $[Na(DME)_n]_2[2]$ by ^1H, ^{11}B and ^{13}C NMR spectroscopy. Purification of this extremely air-sensitive salt by crystallization was not successful. Salts of dicarbadodecaborane dianions are known to be extremely air- and moisture-sensitive.[57] The $^{11}B\{^1H\}$ NMR spectrum recorded in CD_3CN revealed a 2 : 1 : 1 : 2 : 2 : 2 pattern for the cluster atoms and a very broad signal at 67.5 ppm corresponding to the boryl boron atom (Fig. 14). The latter peak is considerably shifted to higher field by about 13 ppm compared to the neutral starting material.

Chemical reductions of the Mes_2B compound **2** in THF with alkali metals were carried out as for **5**. After observation of the purple colours corresponding to the radical species and

the disappearance of the peaks corresponding to the starting material, the clear solutions containing the dianions $[2]^{2-}$ were dark red. ^{11}B NMR spectra of the dianions $[2]^{2-}$ show either a 2 : 1 : 1 : 2 : 2 : 2 (Li salt) or a 2 : 2 : 2 : 2 : 2 (Na, K) peak pattern (Fig. 13) and are similar to peaks found for the diphenylcarborane dianions $[5]^{2-}$ when taking into account the lower symmetry in $[2]^{2-}$.

The similarities in the ^{11}B NMR peaks observed for $[2]^{2-}$ and $[5]^{2-}$ suggest that both have bowl-shaped geometries. Geometry optimisations on the $BMes_2$ species $[2]^{2-}$ reveal that the starting geometry **B** was rearranged to the bowl-shaped geometry **D**. The most stable geometry for $[2]^{2-}$ is **C** with **D** only 0.8 kcal mol^{-1} higher in energy. However, computed ^{11}B NMR shifts from geometry **D** fit better with observed ^{11}B NMR shifts than geometry **C** for $[2]^{2-}$ assuming fluctionalities between mirror-image geometries occur in solution (Fig. 15).

Table 4 Computed and observed $^{11}\text{B}\{^1\text{H}\}$ NMR data of $[2]^{2-}$ and $[5]^{2-}$ in ppm and relative energies of the optimised geometries in kcal mol^{-1}

	Geometry	B3,6	B12	B9	B4,5	B7,11	B8,10	BMes$_2$	Rel. E
$[2]^{2-}$	A[a]								14.0
	C	13.3	−1.2	−8.4	−17.4	−21.3	−23.7	60.2	0.0
	D	−4.1	−10.5	−11.8	−15.4	−19.5	−29.2	56.0	0.8
Exp.[b]		0.1	−9.2	−10.1	−14.0	−17.8	−27.2	67.5	
$[5]^{2-}$	A[c]								11.0
	B	−23.5	−20.0	−20.0	−18.6	−18.6	−55.7		5.5
	C	12.2	−7.6	−7.6	−20.7	−20.7	−25.5		0.0
Exp.[d]		7.0	−9.3	−9.3	−17.3	−17.3	−27.5		

[a] All borons are non-equivalent in geometry **A** of $[2]^{2-}$, values are calculated assuming same fluctionality process as in geometry **A** of $[5]^{2-}$; 64.6 (BMes$_2$), 14.1 (B12), 12.1 (B10), 5.7 (B11), −0.7 (B4), −1.7 (B6), −7.3 (B8), −18.2 (B5), −20.3 (B1), −23.9 (B3), −24.8 (B2). [b] Experimental data for sodium salt in CD$_3$CN, Fig. 14. [c] Calculated values are averaged assuming fluctionality between two mirror-image geometries; 10.0 (B10,12), −0.8 (B11), −6.0 (B8), −9.3 (B5,6), −18.8 (B3), −20.6 (B2,4), −25.6 (B1). [d] Experimental data for sodium salt in d$_8$-THF.
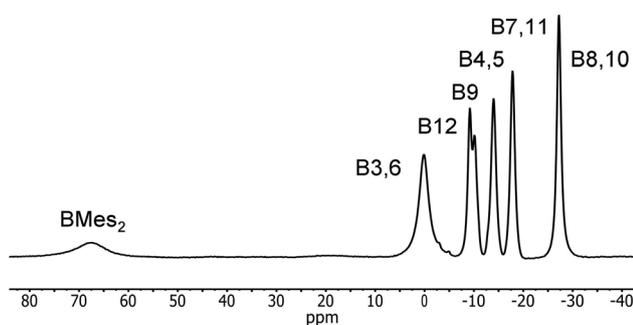

Fig. 14 $^{11}\text{B}\{^1\text{H}\}$ NMR spectrum of $[2]^{2-}$ in CD$_3$CN with peak assignments based on GIAO-NMR data.

It is concluded here that bowl-shaped geometries are present in solutions of 12-vertex *nido*-dicarbadodecaborane dianions with fluctional cluster geometries of **C** and **D** in dia-

nions of *C,C'*-diphenyl-carborane $[5]^{2-}$ and *C*-dimesitylboryl-*C'*-phenyl-carborane $[2]^{2-}$ respectively. The calculated geometries for $[2]^{2-}$ and $[5]^{2-}$ are similar to the experimental cluster geometries[61] of $[9]^{2-}$ and $[8]^{2-}$ respectively as shown from comparison of distances involving the cluster carbon atoms, C1 and C2, in Table 5. The combined experimental and calculated ^{11}B NMR method is shown to be useful in determining *nido*-

Table 5 Comparison of selected distances in Å for the *nido*-dianions, $[2]^{2-}$, $[5]^{2-}$, $[8]^{2-}$ and $[9]^{2-}$

	$[2]^{2-}$ calc.	$[9]^{2-}$ obs.	$[5]^{2-}$ calc.	$[8]^{2-}$ obs.
C1···C2	2.666	2.687(6)	2.915	2.87(1)
C1···B3	2.528	2.302(9)	2.606	2.59(1)
C1···B6	1.624	1.617(9)	1.546	1.51(1)
C2···B3	1.586	1.534(8)	1.546	1.51(1)
C2···B6	1.878	2.083(8)	2.606	2.55(1)
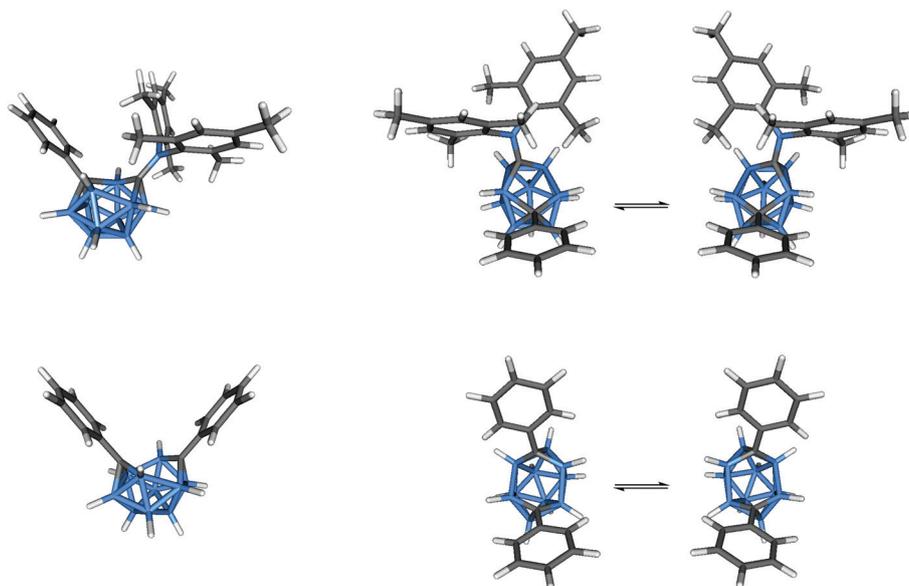
Fig. 15 Optimised geometries of $[2]^{2-}$ (top) and $[5]^{2-}$ (bottom) and the fluctional processes.

12-vertex geometries in solutions and will aid further progress on the intriguing range of *nido*-12-vertex geometries in the future.

Conclusions

Two *C*-dimesitylboryl-1,2-dicarba-*closo*-dodecaboranes were synthesised from fluorodimesitylborane and the corresponding lithio-carboranes and structurally characterised by X-ray crystallography. Photophysical studies and TD-DFT calculations showed that the absorptions correspond to local transitions within the BMes$_2$ groups whereas visible emissions with Stokes shifts up to 16 170 and 14 800 cm^{-1} in dichloromethane originate from intramolecular CT transitions between the mesityl rings and the cluster. Compound **2** with a phenyl substituent at the second cage carbon atom can be easily reduced to a stable dianion [**2**]$^{2-}$ by cyclic voltammetry and chemical reductions with alkali metals. Based on experimental and calculated ^{11}B NMR data, a dynamic bowl-shaped *nido*-cage geometry is determined for the dianion. These findings indicate that the *ortho*-carboranyl group is a stronger electron acceptor than the BMes$_2$ group and *C*-dimesitylboryl-1,2-dicarba-*closo*-dodecaboranes are dyads with the mesityl group as the donor and the carborane as the acceptor.

Experimental section

General

The reactions were performed under an atmosphere of dry oxygen-free argon using Schlenk techniques unless otherwise stated. All solvents were dried by standard methods and freshly distilled prior to use. Fluorodimesitylborane[68] and 1-phenyl-1,2-dicarba-*closo*-dodecaborane[69] were prepared as described in the literature. 1,2-Dicarba-*closo*-dodecaborane was purchased commercially (KatChem). NMR spectra were recorded from solutions at room temperature on a Bruker AM Avance DRX500 (^{1}H, ^{11}B, ^{13}C), a Bruker Avance III 500 and a Bruker Avance 400 Spectrometer (^{1}H{^{11}B}, ^{19}F) with SiMe$_4$ (^{1}H, ^{13}C), BF$_3$·OEt$_2$ (^{11}B) and CFCl$_3$ (^{19}F) as external standards. ^{1}H- and ^{13}C{^{1}H} NMR spectra were calibrated on the solvent signal [CDCl$_3$: 7.24 (^{1}H), 77.16 (^{13}C); CD$_3$CN: 1.94 (^{1}H), 118.25, 1.32 (^{13}C); d$_8$-THF: 3.58, 1.73 (^{1}H), 67.57, 25.46 (^{13}C)]. The ^{13}C NMR peaks were assigned with the aid of observed ^{13}C DEPT spectra and computed ^{13}C NMR shifts. Electron Ionisation (EI) and Atmospheric pressure Solids Analysis Probe (ASAP) mass spectra were recorded with a VG Autospec sector field (Micromass) and Xevo QTOF (Waters) mass spectrometers respectively.

1-Dimesitylboryl-1,2-dicarba-*closo*-dodecaborane (1). A solution of *n*-butyllithium (1.6 M in *n*-hexane, 2.37 mL, 3.79 mmol) was added to 1,2-dicarba-*closo*-dodecaborane (0.52 g, 3.61 mmol) in toluene (35 mL) at 0 °C. After 16 h stirring at ambient temperature a solution of fluorodimesitylborane (0.96 g, 3.58 mmol) in toluene (6 mL) was added to the resulting suspension. The mixture was heated at reflux temperature for 5 h and washed with water (2 × 10 mL) and saturated

sodium chloride solution (10 mL) subsequently. The combined aqueous layers were extracted with toluene (10 mL) and the combined organic phases were dried over sodium sulfate and freed from volatiles *in vacuo*. The crude product was recrystallised from a mixture of *n*-hexane (30 mL) and dichloromethane (2 mL) to afford pure **1** as colourless crystals. Yield: 0.85 g (61%). Found: C, 60.42; H, 8.51; C$_{20}$H$_{33}$B$_{11}$ requires C, 61.22; H, 8.48; ^{1}H-NMR (CDCl$_3$): δ [ppm] = 1.4–3.2 (m, br, 10 H, BH), 2.24 (s, 6 H, *para*-CH$_3$), 2.40 (s, 12 H, *ortho*-CH$_3$), 3.85 (s, br, 1 H, B$_{10}$H$_{10}$C$_2$*H*), 6.80 (s, 4 H, CH$_{Mes}$); ^{13}C{^{1}H}-NMR (CDCl$_3$): δ [ppm] = 20.9 (s, *para*-CH$_3$), 25.9 (s, *ortho*-CH$_3$), 61.6 (s, CB$_{10}$H$_{10}$*C*H), 75.4 (s, CB$_{10}$H$_{10}$*C*BMes$_2$), 129.7 (s, CH$_{Mes}$), 138.4 (s, C$_{ipso}$), 139.4 (s, C$_{ortho}$), 139.8 (s, C$_{para}$); ^{11}B{^{1}H}-NMR (CDCl$_3$): δ [ppm] = −12.9 (s), −9.1 (s), −6.9 (s), −2.3 (s), 1.9 (s) (skeletal boron atoms), 78.9 (s, br, exopolyhedral boron atom) see Fig. S5–S7‡ for NMR spectra of **1**; MS (EI): *m/z* = 392.4 (M$^+$, 3%), 272.3 (M$^+$ − HMes, 51%), 249.2 (BMes$_2^+$, 46%), 120.1 (Mes$^+$, 100%).

1-Dimesitylboryl-2-phenyl-1,2-dicarba-*closo*-dodecaborane (2). A solution of *n*-butyllithium (1.6 M in *n*-hexane, 3.10 mL, 4.96 mmol) was added to 1-phenyl-1,2-dicarba-*closo*-dodecaborane (0.97 g, 4.40 mL) in toluene (40 mL). After stirring for 16 h at ambient temperature a solution of fluorodimesitylborane (1.30 g, 4.85 mmol) in toluene (12 mL) was added and the mixture was heated at reflux temperature for 5 h. Subsequently it was washed with water (2 × 15 mL) and saturated sodium chloride solution (15 mL). The combined organic phases were dried over sodium sulfate and the solvent was removed *in vacuo*. Impurities were sublimed from the residue at 80 °C *in vacuo* and the remaining solid was recrystallised from a mixture of *n*-hexane (80 mL) and dichloromethane (5 mL). The product **2** was obtained as colourless crystals. Yield: 0.97 g (51%). Found: C, 66.38; H, 7.97; C$_{26}$H$_{37}$B$_{11}$ requires C, 66.66; H, 7.96; ^{1}H{^{11}B} NMR (CDCl$_3$): δ [ppm] = 2.16 (s, 6 H, *para*-CH$_3$), 2.26 (s, 14 H, BH + *ortho*-CH$_3$), 2.33 (3H, BH), 2.41 (2H, BH), 2.70 (1H, BH), 3.47 (2H, BH), 6.56 (s, 4 H, CH$_{Mes}$), 6.87 (dd, $^3J_{HH}$ = 7.4 Hz, $^3J_{HH}$ = 7.6 Hz, 2 H, H$_{meta}$), 7.13 (t, $^3J_{HH}$ = 7.4 Hz, 1 H, H$_{para}$), 7.18 (d, $^3J_{HH}$ = 7.6 Hz, 2 H, H$_{ortho}$); ^{13}C{^{1}H} NMR (CDCl$_3$): δ [ppm] = 20.8 (s, *para*-CH$_3$), 26.8 (s, *ortho*-CH$_3$), 86.5 (s, CB$_{10}$H$_{10}$*C*Ph), 87.3 (s, CB$_{10}$H$_{10}$*C*BMes$_2$), 127.7 (s, C$_{meta, Ph}$), 129.3 (s, C$_{para, Ph}$), 129.4 (s, CH$_{Mes}$), 130.3 (s, C$_{ortho, Ph}$), 131.7 (s, C$_{ipso, Ph}$), 138.8 (s, C$_{ipso, Mes}$), 139.1 (s, C$_{para, Mes}$), 139.4 (s, C$_{ortho, Mes}$); ^{11}B{^{1}H} NMR (CDCl$_3$): δ [ppm] = −9.9 (s), −8.0 (s), −2.8 (s), 3.7 (s) (skeletal boron atoms), 80.4 (s, br, exopolyhedral boron atom) see Fig. S8–S10‡ for NMR spectra of **2**; MS (EI): *m/z* = 468.4 (M$^+$, 4%), 453.4 (M$^+$ − Me, 2%), 348.3 (M$^+$ − HMes, 100%), 332.3 (M$^+$ − Me − Mes, 13%), 249.2 (BMes$_2^+$, 85%).

Hydrolyses of 1 and 2

A drop of water (excess) was mixed with a solution of **1** or **2** in deuterated chloroform in an NMR tube and the mixture was analysed by NMR spectroscopy. No change in the spectra was observed after a week.

Hydrolysis by air exposure. Solids of **1** (0.2 g, 0.51 mmol) and **2** (0.3 g, 0.64 mmol) were left exposed to air in the

laboratory and checked periodically by NMR spectroscopy. After three weeks, compound **1** was converted to mesitylene and carboranylboronic acid **3** as determined by multinuclear NMR spectroscopy. After eighteen months, mesitylene and borinic acid **4** were identified as products of **2**.

Mesitylene: ^{1}H-NMR (CDCl$_3$): δ [ppm] = 6.81, 2.25; ^{13}C{^{1}H}-NMR (CDCl$_3$): δ [ppm] = 137.9, 127.0, 21.3.

(1,2-Dicarba-*closo*-dodecaboranyl)-1-borinic acid (**3**): ^{1}H {^{11}B}-NMR (CDCl$_3$): δ [ppm] = 2.05 (2H, BH), 2.17 (2H, BH), 2.26 (2H, BH), 2.33 (4H, BH), 3.67 (1H, B$_{10}$H$_{10}$C$_2$H), 4.91 (2H, OH); ^{13}C{^{1}H}-NMR (CDCl$_3$): δ [ppm] = 57.4 (s, CB$_{10}$H$_{10}$CH), the ^{13}C peak corresponding to CB(OH)$_2$ is not observed; ^{11}B{^{1}H}-NMR (CDCl$_3$): δ [ppm] = −12.6 (s), −7.8 (s), −2.1 (s), −1.0 (s) (skeletal boron atoms), 26.5 (s, exopolyhedral boron atom) see Fig. S11‡ for ^{11}B NMR spectra of **3**; MS (ASAP, M = C$_2$H$_{13}$B$_{11}$O$_2$): m/z = 188.0 (M$^+$, 21%), 171.2 (M$^+$ − OH, 100%).

(2-Phenyl-1,2-dicarba-*closo*-dodecaboranyl)-1-borinic acid (**4**): ^{1}H NMR (CDCl$_3$): δ [ppm] = 2.32 (2H, BH), 2.42 (3H, BH), 2.48 (2H, BH), 2.61 (1H, BH), 2.92 (2H, BH), 4.46 (2H, OH), 7.34 (dd, $^3J_{HH}$ = 7.4 Hz, $^3J_{HH}$ = 7.6 Hz, 2 H, H$_{meta}$), 7.41 (t, $^3J_{HH}$ = 7.4 Hz, 1 H, H$_{para}$), 7.64 (d, $^3J_{HH}$ = 7.6 Hz, 2 H, H$_{ortho}$); ^{13}C{^{1}H} NMR (CDCl$_3$): δ [ppm] = 20.8 (s, *para*-CH$_3$), 26.8 (s, *ortho*-CH$_3$), 86.5 (s, CB$_{10}$H$_{10}$CPh), 87.3 (s, CB$_{10}$H$_{10}$CBMes$_2$), 127.7 (s, C$_{meta, Ph}$), 129.3 (s, C$_{para, Ph}$), 129.4 (s, CH$_{Mes}$), 130.3 (s, C$_{ortho, Ph}$), 131.7 (s, C$_{ipso, Ph}$), 138.8 (s, C$_{ipso, Mes}$), 139.1 (s, C$_{para, Mes}$), 139.4 (s, C$_{ortho, Mes}$); ^{11}B{^{1}H} NMR (CDCl$_3$): δ [ppm] = −11.7 (s), −10.6 (s), −8.3 (s), −3.1 (s), 0.9 (s) (skeletal boron atoms), 26.5 (s, exopolyhedral boron atom) see Fig. S12‡ for ^{11}B NMR spectra of **4**; MS (ASAP, M = C$_8$H$_{17}$B$_{11}$O$_2$): m/z = 263.2 (M − 1$^+$, 44%), 247.2 (M$^+$ − OH, 100%).

Hydrolysis by fluoride ion. 1-Dimesitylboryl-1,2-dicarba-*closo*-dodecaborane (**1**) (0.009 g, 0.023 mmol) was dissolved in a solution of tetra-*n*-butylammonium fluoride trihydrate (0.014 g, 0.044 mmol) in deuterated chloroform (0.8 mL) and the mixture was subject to NMR spectroscopy. Likewise, 1-dimesitylboryl-2-phenyl-1,2-dicarba-*closo*-dodecaborane (**2**) (0.026 g, 0.055 mmol) was dissolved in a deuterated chloroform solution of tetra-*n*-butylammonium fluoride trihydrate (0.018 g, 0.057 mmol). The products identified by multinuclear NMR spectroscopy were dimesitylborinic acid,[37] Mes$_2$BOH, and 1,2-dicarba-*closo*-dodecaborane[70] from **1** and Mes$_2$BOH and 2-phenyl-1,2-dicarba-*closo*-dodecaborane[70] from **2**. Deboronated products were also identified in the reaction mixtures from their NMR data (see Fig. S13‡ for ^{19}F NMR spectra).[40] Dimesitylborinic acid: ^{1}H-NMR (CDCl$_3$): δ [ppm] = 2.30 (12H), 2.32 (6H), 5.97 (1H, OH), 6.86 (4H); ^{13}C{^{1}H}-NMR (CDCl$_3$): δ [ppm] = 21.3, 22.6, 128.5, 137.0, 139.5, 141.2; ^{11}B-NMR (CDCl$_3$): δ [ppm] = 50.1.

Reductions of 2 and 5

Method 1. A piece of excess sodium metal was added to a solution of 1-dimesitylboryl-2-phenyl-1,2-dicarba-*closo*-dodecaborane **2** (0.07 g, 0.14 mmol) in 1,2-dimethoxyethane (0.5 mL). A dark red colour occurred immediately on the surface of the metal. The mixture was sonicated for 1 h and filtered subsequently. The filtrate was freed from volatiles *in vacuo* and the

dark red remainder was taken up in d$_3$-acetonitrile and analysed by NMR spectroscopy. Na$_2$[**2**] ^{1}H NMR (CD$_3$CN): δ [ppm] = −0.4–3.0 (m, br, 10 H, BH), 2.15 (s, 6 H, *para*-CH$_3$), 2.32 (s, 12 H, *ortho*-CH$_3$), 6.52 (s, br, 4 H, CH$_{Mes}$), 6.76 (s, br, 1 H, H$_{para}$), 6.92 (s, br, 2 H, H$_{Ph}$), 7.43 (s, br, 2 H, H$_{Ph}$); ^{13}C{^{1}H} NMR (CD$_3$CN): δ [ppm] = 20.8 (s, *para*-CH$_3$), 25.1 (s, *ortho*-CH$_3$), 70.5 (s, CB$_{10}$H$_{10}$CPh), 106.7 (s, CB$_{10}$H$_{10}$CBMes$_2$), 122.0 (s, CH$_{Ph}$ *para*), 127.6 (br s, CH$_{Mes}$, CH$_{Ph}$ *meta*), 128.7 (s, CH$_{Ph}$ *ortho*), 133.6 (s, s, C$_{Mes}$-*para*), 140.9 (s, C$_{Mes}$-*ortho*), 149.4 (s, C$_{Mes}$-*ipso*), 154.2 (s, C$_{Ph}$ *ipso*); ^{11}B{^{1}H} NMR (CD$_3$CN): δ [ppm] = −27.2 (s), −17.8 (s), −14.0 (s), −10.1 (s), −9.2 (s), 0.1 (s) (skeletal boron atoms), 67.5 (s, br, exopolyhedral boron atom) see Fig. 14; UV-Vis for [**2**]$^{2−}$ in CH$_3$CN, [nm ($ε$)] = 344 (4600), 405 (1700), 430 (1400), 515 (1300) (Fig. S4‡).

Method 2. Finely-cut alkali metal pieces were added to a solution of **2** (0.07 g, 0.14 mmol) in tetrahydrofuran (0.5 mL). A purple colour occurred immediately at the metal surface followed by a clear dark red solution after 2 h. The reaction mixture was then analysed by ^{11}B NMR spectroscopy and in many experiments the desired dianion was present as the carborane compound (Table S5‡). ^{1}H and ^{13}C NMR spectra were also obtained for Na$_2$[**2**] when deuterated THF was used in place of THF. Na$_2$[**2**]. ^{1}H{^{11}B} NMR (d$_8$-THF): δ [ppm] = 0.26 (s, 2 H, BH), 1.16 (s, 2 H, BH), 1.59 (s, 2 H, BH), 2.09 (s, 6 H, *para*-CH$_3$), 2.19 (s, 1 H, BH), 2.35 (s, 12 H, *ortho*-CH$_3$), 6.46 (s, 4 H, CH$_{Mes}$), 6.68 (t, 7.5 Hz, 1 H, H$_{para}$), 6.82 (apparent triplet, ~8 Hz, 2 H, H$_{Ph}$ *meta*), 7.37 (d, 8 Hz, 2 H, H$_{Ph}$ *ortho*); ^{13}C{^{1}H} NMR (d$_8$-THF): 21.3 (s, *para*-CH$_3$), 122.3 (s, CH$_{Ph}$ *para*), 126.7 (s, CH$_{Ph}$ *meta*), 127.7 (s, CH$_{Mes}$), 128.9 (s, CH$_{Ph}$ *ortho*), 133.1 (s, C$_{Mes}$-*para*), 140.8 (s, C$_{Mes}$-*ortho*), 148.7 (s, C$_{Mes}$-*ipso*), 153.5 (s, C$_{Ph}$ *ipso*); the peak corresponding to *ortho*-CH$_3$ groups is hidden within the d$_8$-THF peak and the peaks for the cage carbons were not detected above the noise levels, see Fig. S14 and S15‡ for ^{1}H{^{11}B} and ^{13}C{^{1}H} NMR spectra. Exposing the dark red solution containing Na$_2$[**2**] slowly to air gave a light yellow solution identified by NMR spectroscopy to contain a mixture of the starting material **2** and 1-phenyl-*ortho*-carborane in a 9 : 1 ratio. Method 2 was also used in the reductions of **5** with alkali metals (Li, Na, K) but with deuterated THF in all cases and NMR data of M$_2$[**5**] (M = Li, Na, K) are listed in Table S6.‡

Photophysical measurements

For all solution state measurements, samples were contained in quartz cuvettes of 10 × 10 mm (Hellma type 111-QS, suprasil, optical precision). Cyclohexane was used as received from commercial sources (p.a. quality), the other solvents were dried by standard methods prior to use. Concentrations varied from 20 to 100 μM in order to get analysable emission spectra due to the low quantum yields. Effects of the concentration on the shape of the observed emission spectra were excluded in this concentration range. Solid samples were prepared by vacuum sublimation on quartz plates (35 × 10 × 1 mm) using standard Schlenk equipment and conditions. Each plate was laid in a 100 mL round bottom flask and a crystal of the sample substance placed below it was sublimed. Absorption

was measured with a UV/VIS double-beam spectrometer (Shimadzu UV-2550), using the solvent as a reference.

The output of a continuous Xe-lamp (75 W, LOT Oriel) was wavelength-separated by a first monochromator (Spectra Pro ARC-175, 1800 l mm^{-1} grating, Blaze 250 nm) and then used to irradiate a sample. The fluorescence was collected by mirror optics at right angles and imaged on the entrance slit of a second spectrometer while compensating astigmatism at the same time. The signal was detected by a back-thinned CCD camera (RoperScientific, 1024\256 pixels) in the exit plane of the spectrometer. The resulting images were spatially and spectrally resolved. As the next step, one averaged fluorescence spectrum was calculated from the raw images and stored in the computer. This process was repeated for different excitation wavelengths. The result is a two-dimensional fluorescence pattern with the y-axis corresponding to the excitation, and the x-axis to the emission wavelength. The wavelength range is λ_{ex} = 230–430 nm (in 1 nm increments) for the UV light and λ_{em} = 305–894 nm for the detector. The time to acquire a complete EES is typically less than 15 min. Postprocessing of the EES includes subtraction of the dark current background, conversion of pixel to wavelength scales, and multiplication with a reference file to take the varying lamp intensity as well as grating and detection efficiency into account. Stokes shifts were calculated from excitation and emission maxima, which were extracted from spectra that were converted from wavelength to wavenumbers beforehand. The quantum yields in solution were determined against POPOP (*p*-bis-5-phenyl-oxazolyl(2)-benzene) (Φ_F = 0.93) as the standard.

The solid-state fluorescence was measured by addition of an integrating sphere (Labsphere, coated with Spectralon, Ø 12.5 cm) to the existing experimental setup. At the exit slit of the first monochromator the exciting light was transferred into a quartz fibre (LOT Oriel, LLB592). It passed a condenser lens and illuminated a 1 cm^2 area on the sample in the centre of the sphere. The emission and exciting light was imaged by a second quartz fibre on the entrance slit of the detection monochromator. Post-processing of the spectra was done as described above. The measurement and calculation of quantum yields was performed according to the method described by Mello.[71]

Electrochemistry

Cyclic voltammetric measurements were carried out using an EcoChemie Autolab PG-STAT 30 potentiostat at 298 K with a platinum or glassy carbon working electrode and platinum wires as counter and reference electrodes in a nitrogen-containing glove box with 0.1 M tetra-*n*-butylammonium hexafluorophosphate [Bu$_4$N][PF$_6$] in DCM or acetonitrile. Scan rates of 100 mV s^{-1} and analyte concentrations of 10^{-3} M were used. The ferrocene/ferrocenium FcH/FcH$^+$ couple served as internal reference at 0.0 V for potential measurements and peak–peak separations of this couple were generally in the region of 90–110 mV.

The spectroelectrochemical (SEC) experiment on **2** was performed at room temperature in an airtight optically transparent thin-layer electrochemical (OTTLE) cell[72] equipped with Pt minigrid working and counter electrodes (32 wires cm^{-1}), Ag wire pseudo-reference electrode and CaF$_2$ windows for a 200 μm path-length solvent compartment. Acetonitrile containing 0.1 M [Bu$_4$N][PF$_6$] electrolyte was used in the cell which was fitted into the sample compartment of a Cary 5000 (UV-Vis-NIR) spectrophotometer. Bulk electrolysis was carried out using an Autolab PG-STAT 30 potentiostat.

Crystallographic studies

Single crystals were coated with a layer of hydrocarbon oil and attached to a glass fiber. Crystallographic data were collected with a Bruker AXS X8 Prospector Ultra APEX II diffractometer with Cu Kα radiation (graphite monochromator, λ = 1.54178 Å) at 100 K. Crystallographic programs used for structure solution and refinement were from SHELX-97.[73] The structures were solved by direct methods and were refined by using full-matrix least squares on F^2 of all unique reflections with anisotropic thermal parameters for all non-hydrogen atoms. The hydrogen atoms bonded to the carborane units were refined isotropically, all other hydrogen atoms were refined using a riding model with $U(H)$ = 1.5U_{eq} for CH$_3$ groups and $U(H)$ = 1.2U_{eq} for all others. Crystallographic data for the compounds are listed in Table S7.‡ CCDC 1048027 (**1**) and CCDC 1048028 (**2**) contain the supplementary crystallographic data for this paper.

Computational details

All computations were carried out with the Gaussian 09 package.[74] The model geometries were fully optimised with the B3LYP functional[75] with no symmetry constraints using the 6-31G* basis set[76] for all atoms. Frequency calculations on all optimised geometries revealed no imaginary frequencies. Computed absorption data were obtained from TD-DFT[77] calculations on S$_0$ geometries whereas computed emission data were from the S$_1$ geometries. The MO diagrams and MO compositions were generated with the Molekel[78] and GaussSum[79] packages, respectively. Calculated ^{11}B and ^{13}C NMR chemical shifts obtained at the GIAO[80]-B3LYP/6-31G*//B3LYP/6-31G* level on the optimised geometries were referenced to BF$_3$·OEt$_2$ for ^{11}B: $\delta(^{11}$B) = 111.7–$\sigma(^{11}$B) and referenced to TMS for ^{13}C: $\delta(^{13}$C) = 189.4–$\sigma(^{13}$C). Computed NMR values reported here were averaged where possible.

References

1 (a) C. D. Entwistle and T. B. Marder, *Angew. Chem.*, 2002, **114**, 3051–3056, (*Angew. Chem., Int. Ed.*, 2002, **41**, 2927–2931); (b) C. D. Entwistle and T. B. Marder, *Chem. Mater.*, 2004, **16**, 4574–4585; (c) S. Yamaguchi and A. Wakamiya, *Pure Appl. Chem.*, 2006, **78**, 1413–1424; (d) F. Jäkle, *Coord. Chem. Rev.*, 2006, **250**, 1107–1121.

2 A. Schulz and W. Kaim, *Chem. Ber.*, 1989, **122**, 1863–1868.

3 M. E. Glogowski and J. L. R. Williams, *J. Organomet. Chem.*, 1981, **218**, 137–146.

4 (a) T. Noda and Y. Shirota, *J. Am. Chem. Soc.*, 1998, **120**, 9714–9715; (b) M. Kinoshita, N. Fujii, T. Tsukaki and Y. Shirota, *Synth. Met.*, 2001, **121**, 1571–1572.

5 (a) W.-L. Jia, D.-R. Bai, T. Mc Cormick, Q.-D. Liu, M. Motala, R.-Y. Wang, C. Seward, Y. Tao and S. Wang, *Chem. – Eur. J.*, 2004, **10**, 994–1006; (b) W.-L. Jia, D. Feng, D.-R. Bai, Z. H. Lu, S. Wang and G. Vamvounis, *Chem. Mater.*, 2005, **17**, 164–170; (c) M. Mazzeo, V. Vitale, F. Della Sala, M. Anni, G. Barbarella, L. Favaretto, G. Sotgui, R. Cingolani and G. Gigli, *Adv. Mater.*, 2005, **17**, 34–39.

6 (a) T. Noda, H. Ogawa and Y. Shirota, *Adv. Mater.*, 1999, **11**, 283–285; (b) T. Noda and Y. Shirota, *J. Lumin.*, 2000, **87–89**, 1168–1170; (c) Y. Shirota, M. Kinoshita, T. Noda, K. Okumoto and T. Ohara, *J. Am. Chem. Soc.*, 2000, **122**, 11021–11022; (d) W.-Y. Wong, S.-Y. Poon, M.-F. Lin and W.-K. Wong, *Aust. J. Chem.*, 2007, **60**, 915–922; (e) G.-J. Zhou, G.-L. Ho, W.-Y. Wong, Q. Wang, D.-G. Ma, L.-X. Wang, Z.-Y. Lin, T. B. Marder and A. Beeby, *Adv. Funct. Mater.*, 2008, **18**, 499–511; (f) C.-L. Ho;, B. Yao, B. Zhang, K.-L. Wong, W.-Y. Wong, Z. Xie, L. Wang and Z. Lin, *J. Organomet. Chem.*, 2013, **730**, 144–155.

7 (a) E. Sakuda, A. Funahashi and N. Kitamura, *Inorg. Chem.*, 2006, **45**, 10670–10677; (b) M. Melaimi and F. P. Gabbaï, *J. Am. Chem. Soc.*, 2005, **127**, 9680–9681; (c) Y. Kim and F. P. Gabbaï, *J. Am. Chem. Soc.*, 2009, **131**, 3363–3369; (d) S.-B. Zhao, T. McCormick and S. Wang, *Inorg. Chem.*, 2007, **46**, 10965–10967; (e) M.-S. Yuan, Z.-Q. Liu and Q. Fang, *J. Org. Chem.*, 2007, **72**, 7915–7922; (f) X. Y. Liu, D. R. Bai and S. Wang, *Angew. Chem.*, 2006, **118**, 5601–5604, (*Angew. Chem., Int. Ed.*, 2006, **45**, 5475–5478); (g) D.-R. Bai, X.-Y. Liu and S. Wang, *Chem. – Eur. J.*, 2007, **13**, 5713–5723; (h) M. H. Lee, T. Agou, J. Kobayashi, T. Kawashima and F. P. Gabbaï, *Chem. Commun.*, 2007, 1133–1135; (i) T. W. Hudnall, M. Melaïmi and F. P. Gabbaï, *Org. Lett.*, 2006, **8**, 2747–2749; (j) H.-P. Shi, J.-X. Dai, L. Xu, L.-W. Shi, L. Fang, S.-M. Shuang and C. Dong, *Org. Biomol. Chem.*, 2012, **10**, 3852–3858; (k) C.-W. Chiu and F. P. Gabbaï, *J. Am. Chem. Soc.*, 2006, **128**, 14248–14249; (l) S. Yamaguchi, S. Akiyama and K. Tamao, *J. Am. Chem. Soc.*, 2001, **123**, 11372–11375; (m) S. Yamaguchi, T. Shirasaka, S. Akiyama and K. Tamao, *J. Am. Chem. Soc.*, 2002, **124**, 8816–8817; (n) Y. Kubo, M. Yamamoto, M. Ikeda, M. Takeuchi, S. Shinkai, S. Yamaguchi and K. Tamao, *Angew. Chem.*, 2003, **115**, 2082–2086, (*Angew. Chem., Int. Ed.*, 2003, **42**, 2036–2040); (o) S. Solé and

F. P. Gabbaï, *Chem. Commun.*, 2004, 1284–1285; (p) T. W. Hudnall and F. P. Gabbaï, *J. Am. Chem. Soc.*, 2007, **129**, 11978–11986; (q) A. Sundararaman, M. Victor, R. Varughese and F. Jäkle, *J. Am. Chem. Soc.*, 2005, **127**, 13748–13749; (r) K. Parab, K. Venkatasubbaiah and F. Jäkle, *J. Am. Chem. Soc.*, 2006, **128**, 12879–12885; (s) W.-J. Xu, S.-H. Liu, X. Zhao, N. Zhao, X.-Q. Yu and W. Huang, *Chem. – Eur. J.*, 2013, **19**, 621–629; (t) Z. Zhang, R. M. Edkins, J. Nitsch, K. Fucke, A. Eichhorn, A. Steffen, Y. Wang and T. B. Marder, *Chem. – Eur. J.*, 2015, **21**, 177–190.

8 L. Weber, D. Eickhoff, J. Kahlert, L. Böhling, A. Brockhinke, H.-G. Stammler, B. Neumann and M. A. Fox, *Dalton Trans.*, 2012, **41**, 10328–10346.

9 S.-B. Zhao, P. Wucher, Z. M. Hudson, T. M. McCormick, X.-Y. Liu, S. Wang, X.-D. Feng and Z.-H. Lu, *Organometallics*, 2008, **27**, 6446–6456.

10 (a) Y. Kim, H.-S. Huh, M. H. Lee, I. L. Lenov, H. Zhao and F. P. Gabbaï, *Chem. – Eur. J.*, 2011, **17**, 2057–2062; (b) C. Wang, J. Jia, W.-N. Zhang, H.-Y. Zhang and C. H. Zhao, *Chem. – Eur. J.*, 2014, **17**, 16590–16601; (c) J. Jia, P. Xue, Y. Zhang, Q. Xu, G. Zhang, T. Huang, H. Zhang and R. Lu, *Tetrahedron*, 2014, **70**, 5499–5504.

11 C. Bresner, C. J. E. Haynes, D. A. Addy, A. E. J. Broomsgrove, P. Fitzpatrick, D. Vidovic, A. L. Thompson, I. A. Fallis and S. Aldridge, *New J. Chem.*, 2010, **34**, 1652–1659.

12 R. N. Grimes, *Carboranes*, Academic Press (Elsevier), New York, 2nd edn, 2011.

13 For other reviews on carboranes see: (a) B. P. Dash, R. Satapathy, J. A. Maguire and N. S. Hosmane, *New J. Chem.*, 2011, **35**, 1955–1972; (b) I. B. Sivaev and V. V. Bregadze, *Eur. J. Inorg. Chem.*, 2009, 1433–1450; (c) F. Issa, M. Kassiou and L. M. Rendina, *Chem. Rev.*, 2011, **111**, 5701–5722; (d) M. Scholz and E. Hey-Hawkins, *Chem. Rev.*, 2011, **111**, 7035–7062; (e) J. F. Valliant, K. J. Guenther, A. S. King, P. Morel, P. Schaffer, O. O. Sogbein and K. A. Stephenson, *Coord. Chem. Rev.*, 2002, **232**, 173–230; (f) V. N. Kalinin and V. A. Ol'shevskaya, *Russ. Chem. Bull.*, 2008, **57**, 815–836; (g) V. I. Bregadze, *Chem. Rev.*, 1992, **92**, 209–223; (h) A. F. Armstrong and J. F. Valliant, *Dalton Trans.*, 2007, 4240–4251; (i) L. A. Leites, *Chem. Rev.*, 1992, **92**, 279–323; (j) T. J. Wedge and M. F. Hawthorne, *Coord. Chem. Rev.*, 2003, **240**, 111–128; (k) D. Olid, C. Viñas and F. Teixidor, *Chem. Soc. Rev.*, 2013, **42**, 3318–3336; (l) C. Viñas, R. Núñez and F. Teixidor, Large molecules containing icosahedral boron clusters designed for potential applications, in *Boron Science*, ed. N. S. Hosmane, CRC Press, New York, 2012, ch. 27.

14 (a) B. P. Dash, R. Satapathy, J. A. Maguire and N. S. Hosmane, *Chem. Commun.*, 2009, 3267–3269; (b) Y. A. Kabachii and P. M. Valetskii, *Int. J. Polym. Mater.*, 1990, **14**, 9–19; (c) K. Hideaki, O. Koichi, I. Motokuni, S. Toshiya, K. Shigeki and A. Isao, *Chem. Mater.*, 2003, **15**, 355–362; (d) E. Hao, B. Fabre, F. R. Fronczek and M. G. H. Vicente, *Chem. Commun.*, 2007, 4387–4389; (e) E. Hao, B. Fabre, F. R. Fronczek and M. G. H. Vicente,

Chem. Mater., 2007, **19**, 6195–6205; (*f*) M. A. Fox and K. Wade, *J. Mater. Chem.*, 2002, **12**, 1301–1306; (*g*) O. K. Farha, A. M. Spokoyny, K. L. Mulfort, M. F. Hawthorne, C. A. Mirkin and J. T. Hupp, *J. Am. Chem. Soc.*, 2007, **129**, 12680–12681.

15 (*a*) J. Llop, C. Viñas, J. M. Oliva, F. Teixidor, M. A. Flores, R. Kivekäs and R. Sillanpää, *J. Organomet. Chem.*, 2002, **657**, 232–238; (*b*) J. M. Oliva, N. L. Allan, P. v. R. Schleyer, C. Viñas and F. Teixidor, *J. Am. Chem. Soc.*, 2005, **127**, 13538–13547; (*c*) D. A. Brown, W. Clegg, H. M. Colquhoun, J. A. Daniels, I. R. Stephenson and K. Wade, *J. Chem. Soc., Chem. Commun.*, 1987, 889–891; (*d*) L. A. Boyd, W. Clegg, R. C. B. Copley, M. G. Davidson, M. A. Fox, T. G. Hibbert, J. A. K. Howard, A. Mackinnon, R. J. Peace and K. Wade, *Dalton Trans.*, 2004, 2786–2799.

16 (*a*) T. D. Getman, C. B. Knobler and M. F. Hawthorne, *J. Am. Chem. Soc.*, 1990, **112**, 4593–4594; (*b*) T. D. Getman, C. B. Knobler and M. F. Hawthorne, *Inorg. Chem.*, 1992, **31**, 101–105.

17 For recent articles and seminal reviews on *ortho*-carborane derivatives, see: (*a*) S. V. Svidlov, O. A. Varzatskii, T. V. Potapova, A. V. Vologzhanina, S. S. Bukalov, L. A. Leites, Y. Z. Voloshin and Y. N. Bubnov, *Inorg. Chem. Commun.*, 2014, **43**, 142–145; (*b*) J. Marshall, J. Hooton, Y. Han, A. Creamer, R. S. Ashraf, Y. Porte, T. D. Anthopoulos, P. N. Stavrinou, M. A. McLachlan, H. Bronstein, P. Beavis and M. Heeney, *Polym. Chem.*, 2014, **5**, 6190–6199; (*c*) J. Marshall, Z. Fei, C. P. Yau, N. Yaacobi-Gross, S. Rossbauer, T. D. Anthopoulos, S. E. Watkins, P. Beavis and M. Heeney, *J. Mater. Chem. C*, 2014, **2**, 232–239; (*d*) J. Fajardo, A. L. Chan, F. S. Tham and V. Lavallo, *Inorg. Chim. Acta*, 2014, **422**, 206–208; (*e*) B. Wrackmeyer, E. V. Klimkina and W. Milius, *Eur. J. Inorg. Chem.*, 2014, 233–246; (*f*) Z. Qiu, *Tetrahedron Lett.*, 2015, **56**, 963–971; (*g*) J. U. Kahlert, A. Rawal, J. M. Hook, L. M. Rendina and M. Choucair, *Chem. Commun.*, 2014, **50**, 11332–11334; (*h*) M. E. El-Zaria, K. Keskar, A. R. Genady, J. A. Ioppolo, J. McNulty and J. F. Valliant, *Angew. Chem., Int. Ed.*, 2014, **53**, 5156–5160; (*i*) K. Junold, J. A. Baus, C. Burschka, M. Finze and R. Tacke, *Eur. J. Inorg. Chem.*, 2014, 5099–5102; (*j*) R. N. Grimes, *Dalton Trans.*, 2015, **44**, 5939–5956; (*k*) J. M. Ludlow III, M. Tominaga, Y. Chujo, A. Schultz, X. Lu, T. Xie, K. Guo, C. N. Moorefield, C. Wesdemiotis and G. R. Newkome, *Dalton Trans.*, 2014, **43**, 9604–9611; (*l*) A. Kreienbrink, M. B. Sárosi, R. Kuhnert, P. Wonneberger, A. I. Arkhypchuk, P. Lönnecke, S. Ott and E. Hey-Hawkins, *Chem. Commun.*, 2015, **51**, 836–838; (*m*) Y. Quan and Z. Xie, *J. Am. Chem. Soc.*, 2015, **137**, 3502–3505; (*n*) Y. Nie, Y. Wang, J. Miao, D. Bian, Z. Zhang, Y. Cui and G. Sun, *Dalton Trans.*, 2014, **43**, 5083–5094; (*o*) V. I. Bregadze, *Russ. Chem. Bull.*, 2014, **63**, 1021–1026; (*p*) K. Cao, Y. Huang, J. Yang and J. Wu, *Chem. Commun.*, 2015, **51**, 7257–7260.

18 (*a*) V. Z. Paschenko, R. P. Evstigneeva, V. V. Gorokhov, V. N. Luzgina, V. B. Tusov and A. B. Rubin, *J. Photochem. Photobiol., B*, 2000, **54**, 162–167; (*b*) V. N. Luzgina,

V. A. Ol'shevskaya, A. V. Sekridova, A. F. Mironov, V. N. Kalinin, V. Z. Pashchenko, V. V. Gorokhov, V. B. Tusov and A. A. Shtil', *Russ. J. Org. Chem.*, 2007, **43**, 1243–1251; (*c*) B. P. Dash, R. Satapathy, E. R. Galliard, K. M. Norton, J. A. Maguire, N. Chug and N. S. Hosmane, *Inorg. Chem.*, 2011, **50**, 5485–5493; (*d*) A. Ferrer-Ugalde, E. J. Juárez-Pérez, F. Teixidor, C. Viñas, R. Sillanpää, E. Pérez-Inestrosa and R. Núñez, *Chem. – Eur. J.*, 2012, **18**, 544–553; (*e*) L. Zhu, W. Lv, S. Liu, H. Yan, Q. Zhao and W. Huang, *Chem. Commun.*, 2013, **49**, 10638–10640; (*f*) A. Ferrer-Ugalde, A. González-Campo, C. Viñas, J. Rodriguez-Romero, R. Santillan, N. Farfán, R. Sillanpää, A. Sousa-Pedrares, R. Núñez and F. Teixidor, *Chem. – Eur. J.*, 2014, **20**, 9940–9951; (*g*) G. F. Jin, Y.-J. Cho, K.-R. Wee, S. A. Hong, I.-H. Suh, H.-J. Son, J.-D. Lee, W.-S. Han, D. W. Cho and S. O. Kang, *Dalton Trans.*, 2015, **44**, 2780–2787.

19 (*a*) K. Kokado and Y. Chujo, *Macromolecules*, 2009, **42**, 1418–1420; (*b*) K. Kokado, Y. Tokoro and Y. Chujo, *Macromolecules*, 2009, **42**, 9238–9242; (*c*) K. Kokado, A. Nagai and Y. Chujo, *Macromolecules*, 2010, **43**, 6463–6468; (*d*) K. Kokado and Y. Chujo, *Polym. J.*, 2010, **42**, 363–367; (*e*) K. Kokado, A. Nagai and Y. Chujo, *Tetrahedron Lett.*, 2011, **52**, 293–296; (*f*) K. Kokado and Y. Chujo, *Dalton Trans.*, 2011, **40**, 1919–1923; (*g*) K. Kokado and Y. Chujo, *J. Org. Chem.*, 2011, **76**, 316–319; (*h*) M. Tominaga, H. Naito, Y. Morisaki and Y. Chujo, *Asian J. Org. Chem.*, 2014, **3**, 624–631; (*i*) M. Tominaga, H. Naito, Y. Morisaki and Y. Chujo, *New J. Chem.*, 2014, **38**, 5686–5690.

20 (*a*) K.-R. Wee, W.-S. Han, D. W. Cho, S. Kwon, C. Pac and S. O. Kang, *Angew. Chem.*, 2012, **124**, 2731–2734, (*Angew. Chem., Int. Ed.*, 2012, **51**, 2677–2680); (*b*) S. Kwon, K.-R. Wee, Y.-J. Cho and S. O. Kang, *Chem. – Eur. J.*, 2014, **20**, 5953–5960.

21 S. Inagi, K. Hosoi, T. Kubo, N. Shida and T. Fuchigami, *Electrochemistry*, 2013, **81**, 368–370.

22 (*a*) M. Eo, M. H. Park, T. Kim, Y. Do and M. H. Lee, *Polymer*, 2013, **54**, 6321–6328; (*b*) H. J. Bae, H. Kim, K. M. Lee, T. Kim, Y. S. Lee, Y. Do and M. H. Lee, *Dalton Trans.*, 2014, **43**, 4978–4985; (*c*) H. Naito, Y. Morisaki and Y. Chujo, *Angew. Chem.*, 2015, **127**, 5173–5176, (*Angew. Chem., Int. Ed.*, 2015, **54**, 5084–5087).

23 (*a*) A. R. Davis, J. J. Peterson and K. R. Carter, *ACS Macro Lett.*, 2012, **1**, 469–472; (*b*) J. J. Peterson, A. R. Davis, M. Werre, E. B. Coughlin and K. R. Carter, *ACS Appl. Mater. Interfaces*, 2011, **3**, 1796–1799; (*c*) J. J. Peterson, M. Werre, Y. C. Simon, E. B. Coughlin and K. R. Carter, *Macromolecules*, 2009, **42**, 8594–8598.

24 L. Weber, J. Kahlert, R. Brockhinke, L. Böhling, A. Brockhinke, H.-G. Stammler, B. Neumann, R. A. Harder and M. A. Fox, *Chem. – Eur. J.*, 2012, **18**, 8347–8357.

25 L. Weber, J. Kahlert, L. Böhling, A. Brockhinke, H.-G. Stammler, B. Neumann, R. A. Harder, P. J. Low and M. A. Fox, *Dalton Trans.*, 2013, **42**, 2266–2281.

26 L. Weber, J. Kahlert, R. Brockhinke, L. Böhling, J. Halama, A. Brockhinke, H.-G. Stammler, B. Neumann, C. Nervi, R. A. Harder and M. A. Fox, *Dalton Trans.*, 2013, **42**, 10982–10996.

27 K.-R. Wee, Y.-J. Cho, J. K. Song and S. O. Kang, *Angew. Chem.*, 2013, **125**, 9864–9867, (*Angew. Chem., Int. Ed.*, 2013, **52**, 9682–9685).

28 K.-R. Wee, Y.-J. Cho, S. Jeong, S. Kwon, J.-D. Lee, I.-H. Suh and S. O. Kang, *J. Am. Chem. Soc.*, 2012, **134**, 17982–17990.

29 J. O. Huh, H. Kim, K. M. Lee, Y. S. Lee, Y. Do and M. H. Lee, *Chem. Commun.*, 2010, **46**, 1138–1140.

30 K. C. Song, H. Kim, K. M. Lee, Y. S. Lee, Y. Do and M. H. Lee, *Dalton Trans.*, 2013, **42**, 2351–2354.

31 Z. Yuan, C. D. Entwistle, J. C. Collings, D. Albesa-Jove, A. S. Batsanov, J. A. K. Howard, H. M. Kaiser, D. E. Kaufmann, S.-Y. Poon, W.-Y. Wong, C. Jardin, S. Fatallah, A. Boucekkine, J.-F. Halet and T. B. Marder, *Chem. – Eur. J.*, 2006, **12**, 2758–2771.

32 (*a*) J. L. Boone, R. J. Brotherton and L. L. Petterson, *Inorg. Chem.*, 1965, **4**, 910–912; (*b*) Y. Z. Voloshin, S. Y. Erdyakov, I. G. Makarenko, E. G. Lebed', T. V. Potapova, S. V. Svidlov, Z. A. Starikova, E. V. Pol'shin, M. E. Gurskii and Y. N. Bubnov, *Russ. Chem. Bull.*, 2007, **56**, 1787–1794; (*c*) S. Y. Erdyakov, Y. Z. Voloshin, I. G. Makarenko, E. G. Lebed, T. V. Potapova, A. V. Ignatenko, A. V. Vologzhanina, M. E. Gurskii and Y. N. Bubnov, *Inorg. Chem. Commun.*, 2009, **12**, 135–139; (*d*) K. Ohta, T. Goto, H. Yamazaki, F. Pichierri and Y. Endo, *Inorg. Chem.*, 2007, **46**, 3966–3970.

33 D. A. Brown, H. M. Colquhoun, J. A. Daniels, J. A. H. MacBride, I. R. Stephenson and K. Wade, *J. Mater. Chem.*, 1992, **2**, 793–804.

34 G. Zi, H.-W. Li and Z. Xie, *Organometallics*, 2002, **21**, 3850–3855.

35 (*a*) G. Zi, H.-W. Li and Z. Xie, *Organometallics*, 2002, **21**, 1136–1145; (*b*) Y. Nie, J. Miao, H. Wadepohl, H. Pritzkow, T. Oeser and W. Siebert, *Z. Anorg. Allg. Chem.*, 2013, **639**, 1188–1193.

36 Y. Nie, J. Miao, H. Pritzkow, H. Wadepohl and W. Siebert, *J. Organomet. Chem.*, 2013, **747**, 174–177.

37 N. M. D. Brown, F. Davidson, R. McMullan and J. W. Wilson, *J. Organomet. Chem.*, 1980, **193**, 271–282.

38 R. Anulewicz-Ostrowska, S. Luliński, J. Serwatowski and K. Suwińska, *Inorg. Chem.*, 2000, **39**, 5763–5767.

39 H. C. Brown and V. H. Dodson, *J. Am. Chem. Soc.*, 1957, **79**, 2302–2306.

40 (*a*) H. Tomita, H. Luu and T. Onak, *Inorg. Chem.*, 1991, **30**, 812–815; (*b*) M. A. Fox, J. A. H. MacBride and K. Wade, *Polyhedron*, 1997, **16**, 2449–2507; (*c*) J. Yoo, J.-W. Hwang and Y. Do, *Inorg. Chem.*, 2001, **40**, 568–570.

41 (*a*) J. J. Eisch, B. Shafii, J. D. Odom and A. L. Rheingold, *J. Am. Chem. Soc.*, 1990, **112**, 1847–1853; (*b*) M. H. Chisholm, K. Folting, S. T. Haubrich and J. D. Martin, *Inorg. Chim. Acta*, 1993, **213**, 17–24.

42 D. C. Busby and M. F. Hawthorne, *Inorg. Chem.*, 1982, **21**, 4101–4103.

43 Z. G. Lewis and A. J. Welch, *Acta Crystallogr., Sect. C: Cryst. Struct. Commun.*, 1993, **49**, 705–710.

44 A search in the CCDC database in May 2012 revealed that 95% of the B–C_{Mes} bond lengths in 37 structures of *p*-substituted dimesitylborylbenzene derivatives are in the range of 1.55 Å–1.61 Å. The interplanar angles between the mesityl rings and the planes defined by the boryl-boron atom and the three neighbouring carbon atoms were found between 42.9° and 67.5° in these structures.

45 (*a*) T. D. McGrath and A. J. Welch, *Acta Crystallogr., Sect. C: Cryst. Struct. Commun.*, 1995, **51**, 646–649; (*b*) E. S. Alekseyeva, M. A. Fox, J. A. K. Howard, J. A. H. MacBride and K. Wade, *Appl. Organomet. Chem.*, 2003, **17**, 499–508.

46 S. Schwedler, D. Eickhoff, R. Brockhinke, D. Cherian, L. Weber and A. Brockhinke, *Phys. Chem. Chem. Phys.*, 2011, **13**, 9301–9310.

47 (*a*) E. Lippert, *Z. Naturforsch., A: Phys. Sci.*, 1955, **10**, 541–545; (*b*) E. Lippert, *Z. Elektrochem.*, 1957, **61**, 962–975; (*c*) N. Mataga, Y. Kaifu and M. Koizumi, *Bull. Chem. Soc. Jpn.*, 1955, **28**, 690–691; (*d*) N. Mataga, Y. Kaifu and M. Koizumi, *Bull. Chem. Soc. Jpn.*, 1956, **29**, 465–470; (*e*) G. Weber and F. J. Farris, *Biochemistry*, 1979, **18**, 3075–3078; (*f*) A. C. Benniston, A. Harriman and J. P. Rostron, *Phys. Chem. Chem. Phys.*, 2005, **7**, 3041–3047.

48 L. Weber, D. Eickhoff, T. B. Marder, M. A. Fox, P. J. Low, A. D. Dwyer, D. J. Tozer, S. Schwedler, A. Brockhinke, H.-G. Stammler and B. Neumann, *Chem. – Eur. J.*, 2012, **18**, 1369–1382.

49 (*a*) M. V. Yarosh, T. V. Baranova, V. L. Shirokii, A. A. Érdman and N. A. Maier, *Elektrokhimiya*, 1993, **29**, 921–922. (Russian; English version *Russ. J. Electrochem.*, 1993, **29**, 789–790); (*b*) M. V. Yarosh, T. V. Baranova, V. L. Shirokii, A. A. Érdman and N. A. Maier, *Elektrokhimiya*, 1994, **30**, 406–408. (Russian; English version *Russ. J. Electrochem.*, 1994, **30**, 366–368).

50 R. A. Harder, J. A. H. MacBride, G. P. Rivers, D. S. Yufit, A. E. Goeta, J. A. K. Howard, K. Wade and M. A. Fox, *Tetrahedron*, 2014, **70**, 5182–5189.

51 M. A. Fox, C. Nervi, A. Crivello and P. J. Low, *Chem. Commun.*, 2007, 2372–2374.

52 H. Tricas, M. Colon, D. Ellis, S. A. Macgregor, D. McKay, G. M. Rosair, A. J. Welch, I. V. Glukhov, F. Rossi, F. Laschi and P. Zanello, *Dalton Trans.*, 2011, **40**, 4200–4211.

53 (*a*) M. A. Fox, C. Nervi, A. Crivello, A. S. Batsanov, J. A. K. Howard, K. Wade and P. J. Low, *J. Solid State Electrochem.*, 2009, **13**, 1483–1495; (*b*) G. F. Jin, J.-H. Hwang, J.-D. Lee, K.-R. Wee, I.-H. Suh and S. O. Kang, *Chem. Commun.*, 2013, **49**, 9398–9400; (*c*) J. Kahlert, H.-G. Stammler, B. Neumann, R. A. Harder, L. Weber and M. A. Fox, *Angew. Chem.*, 2014, **126**, 3776–3779, (*Angew. Chem., Int. Ed.*, 2014, **53**, 3702–3705).

54 K. Hosoi, S. Inagi, T. Kubo and T. Fuchigami, *Chem. Commun.*, 2011, **47**, 8632–8634.

55 (*a*) A. V. Lebedev, A. V. Buchtiarov, N. N. Golyshin, Y. G. Kudryatsev, I. Y. Lovchinovsky and L. N. Rozhkov, *Organomet. Chem. USSR*, 1991, **4**, 205–208. (English

Transl.); (*b*) A. V. Lebedev, A. V. Bukhtiarov, Y. G. Kudryavtev and I. N. Rozhkov, *Organomet. Chem. USSR*, 1991, **4**, 208–212. (English Transl.); (*c*) A. V. Bukhtiarov, V. N. Golyshin, A. V. Lebedev, Y. G. Kudryavtsev, I. A. Rodnikov, L. I. Zakharkin and O. V. Kuz'min, *Dokl. Acad. Sci. USSR*, 1989, 45–48. (English Transl.).

56 M. A. Fox, Polyhedral Carboranes, in *Comprehensive Organometallic Chemistry III*, ed. R. H. Crabtree and D. M. P. Mingos, Elsevier, Oxford, 2007, ch. 3.02.

57 K. Chui, H.-W. Li and Z. Xie, *Organometallics*, 2000, **19**, 5447–5453.

58 (*a*) G. Zi, H.-W. Li and Z. Xie, *Organometallics*, 2001, **20**, 3836–3838; (*b*) G. Zi, H.-W. Li and Z. Xie, *Chem. Commun.*, 2001, 1110–1111.

59 G. Zi, H.-W. Li and Z. Xie, *Organometallics*, 2002, **21**, 5415–5427.

60 (*a*) M.-S. Cheung, H.-S. Chan and Z. Xie, *Organometallics*, 2004, **23**, 517–526; (*b*) H. Shen, H.-S. Chan and Z. Xie, *Organometallics*, 2006, **25**, 2617–2625; (*c*) L. Deng, H.-S. Chan and Z. Xie, *Inorg. Chem.*, 2007, **46**, 2716–2724.

61 L. Deng, M.-S. Cheung, H.-S. Chen and Z. Xie, *Organometallics*, 2005, **24**, 6244–6249.

62 (*a*) T. L. Venable, R. B. Maynard and R. N. Grimes, *J. Am. Chem. Soc.*, 1984, **106**, 6187–6193; (*b*) J. T. Spencer, M. R. Pourian, R. J. Butcher, E. Sinn and R. N. Grimes, *Organometallics*, 1987, **6**, 335–343; (*c*) N. S. Hosmane, T. J. Colacot, H. Zhang, J. Yang, J. A. Maguire, Y. Wang, M. B. Ezhova, A. Franken, T. Demissie, K.-J. Lu, D. Zhu, J. L. C. Thomas, J. D. Collins, T. G. Gray, S. N. Hosmane and W. N. Lipscomb, *Organometallics*, 1998, **17**, 5294–5309.

63 J. P. H. Charmant, M. F. Haddow, R. Mistry, N. C. Norman, A. G. Orpen and P. G. Pringle, *Dalton Trans.*, 2008, 1409–1411.

64 (*a*) M. Bühl and P. v. R. Schleyer, *J. Am. Chem. Soc.*, 1992, **114**, 477–491; (*b*) P. v. R. Schleyer, J. Gauss, M. Bühl, R. Greatrex and M. A. Fox, *J. Chem. Soc., Chem. Commun.*, 1993, 1766–1768; (*c*) C. E. Willans, C. A. Kilner and M. A. Fox, *Chem. – Eur. J.*, 2010, **16**, 10644–10648.

65 S. Zlatogorsky, D. Ellis, G. M. Rosair and A. J. Welch, *Chem. Commun.*, 2007, 2178–2180.

66 J. Zhang, X. Fu, Z. Lin and Z. Xie, *Inorg. Chem.*, 2015, **54**, 1965–1973.

67 (*a*) L. I. Zakharkin, V. N. Kalinin and L. S. Podvisotskaya, *Bull. Acad. Sci. USSR Div. Chem. Sci.*, 1966, 1444. (English Transl.); (*b*) L. I. Zakharkin, V. N. Kalinin and L. S. Podvisotskaya, *Bull. Acad. Sci. USSR Div. Chem. Sci.*, 1967, 2212–2217. (English Transl.); (*c*) L. I. Zakharkin, *Pure Appl. Chem.*, 1972, **29**, 513–526; (*d*) L. I. Zakharkin, V. N. Kalinin, V. A. Antonovich and E. G. Rhys, *Bull. Acad.*

Sci. USSR Div. Chem. Sci., 1976, 1009–1014. (English Transl.).

68 A. Pelter, K. Smith and H. C. Brown, *Borane Reagents*, Academic Press, London, 1988, p. 428.

69 L. I. Zakharkin, V. I. Bregadze and O. Y. Okhlobystin, *J. Organomet. Chem.*, 1966, **6**, 228–234.

70 E. S. Alekseyeva, A. S. Batsanov, L. A. Boyd, M. A. Fox, T. G. Hibbert, J. A. K. Howard, J. A. H. MacBride, A. Mackinnon and K. Wade, *Dalton Trans.*, 2003, 475–482.

71 J. C. de Mello, H. F. Wittmann and R. H. Friend, *Adv. Mater.*, 1997, **9**, 230–232.

72 M. Krejcik, M. Danek and F. Hartl, *J. Electroanal. Chem.*, 1991, **317**, 179–187.

73 G. M. Sheldrick, *Acta Crystallogr., Sect. A: Fundam. Crystallogr.*, 2008, **64**, 112–122.

74 M. J. Frisch, G. W. Trucks, H. B. Schlegel, G. E. Scuseria, M. A. Robb, J. R. Cheeseman, G. Scalmani, V. Barone, B. Mennucci, G. A. Petersson, H. Nakatsuji, M. Caricato, X. Li, H. P. Hratchian, A. F. Izmaylov, J. Bloino, G. Zheng, J. L. Sonnenberg, M. Hada, M. Ehara, K. Toyota, R. Fukuda, J. Hasegawa, M. Ishida, T. Nakajima, Y. Honda, O. Kitao, H. Nakai, T. Vreven Jr., J. A. Montgomery, J. E. Peralta, F. Ogliaro, M. Bearpark, J. J. Heyd, E. Brothers, K. N. Kudin, V. N. Staroverov, R. Kobayashi, J. Normand, K. Raghavachari, A. Rendell, J. C. Burant, S. S. Iyengar, J. Tomasi, M. Cossi, N. Rega, J. M. Millam, M. Klene, J. E. Knox, J. B. Cross, V. Bakken, C. Adamo, J. Jaramillo, R. Gomperts, R. E. Stratmann, O. Yazyev, A. J. Austin, R. Cammi, C. Pomelli, J. W. Ochterski, R. L. Martin, K. Morokuma, V. G. Zakrzewski, G. A. Voth, P. Salvador, J. J. Dannenberg, S. Dapprich, A. D. Daniels, O. Farkas, J. B. Foresman, J. V. Ortiz, J. Cioslowski and D. J. Fox, *GAUSSIAN 09 (Revision A.02)*, Gaussian, Inc., Wallingford CT, 2009.

75 (*a*) A. D. Becke, *J. Chem. Phys.*, 1993, **98**, 5648–5652; (*b*) C. Lee, W. Yang and R. G. Parr, *Phys. Rev. B: Condens. Matter*, 1988, **37**, 785–789.

76 (*a*) G. A. Petersson and M. A. Al-Laham, *J. Chem. Phys.*, 1991, **94**, 6081–6090; (*b*) G. A. Petersson, A. Bennett, T. G. Tensfeldt, M. A. Al-Laham, W. A. Shirley and J. Mantzaris, *J. Chem. Phys.*, 1988, **89**, 2193–2218.

77 E. Runge and E. K. U. Gross, *Phys. Rev. Lett.*, 1984, **52**, 997–1000.

78 U. Varetto, *MOLEKEL Version*, Swiss National Supercomputing Centre, Mann, Switzerland.

79 N. M. O'Boyle, A. L. Tenderholt and K. M. Langner, *J. Comput. Chem.*, 2008, **29**, 839–845.

80 (*a*) R. Ditchfield, *Mol. Phys.*, 1974, **27**, 789–807; (*b*) C. M. Rohling, L. C. Allen and R. Ditchfield, *Chem. Phys.*, 1984, **87**, 9–15; (*c*) K. Wolinski, J. F. Hinton and P. Pulay, *J. Am. Chem. Soc.*, 1990, **112**, 8251–8260.